



Neutrinoless double beta decay with EXO-200

Yung-Ruey Yen

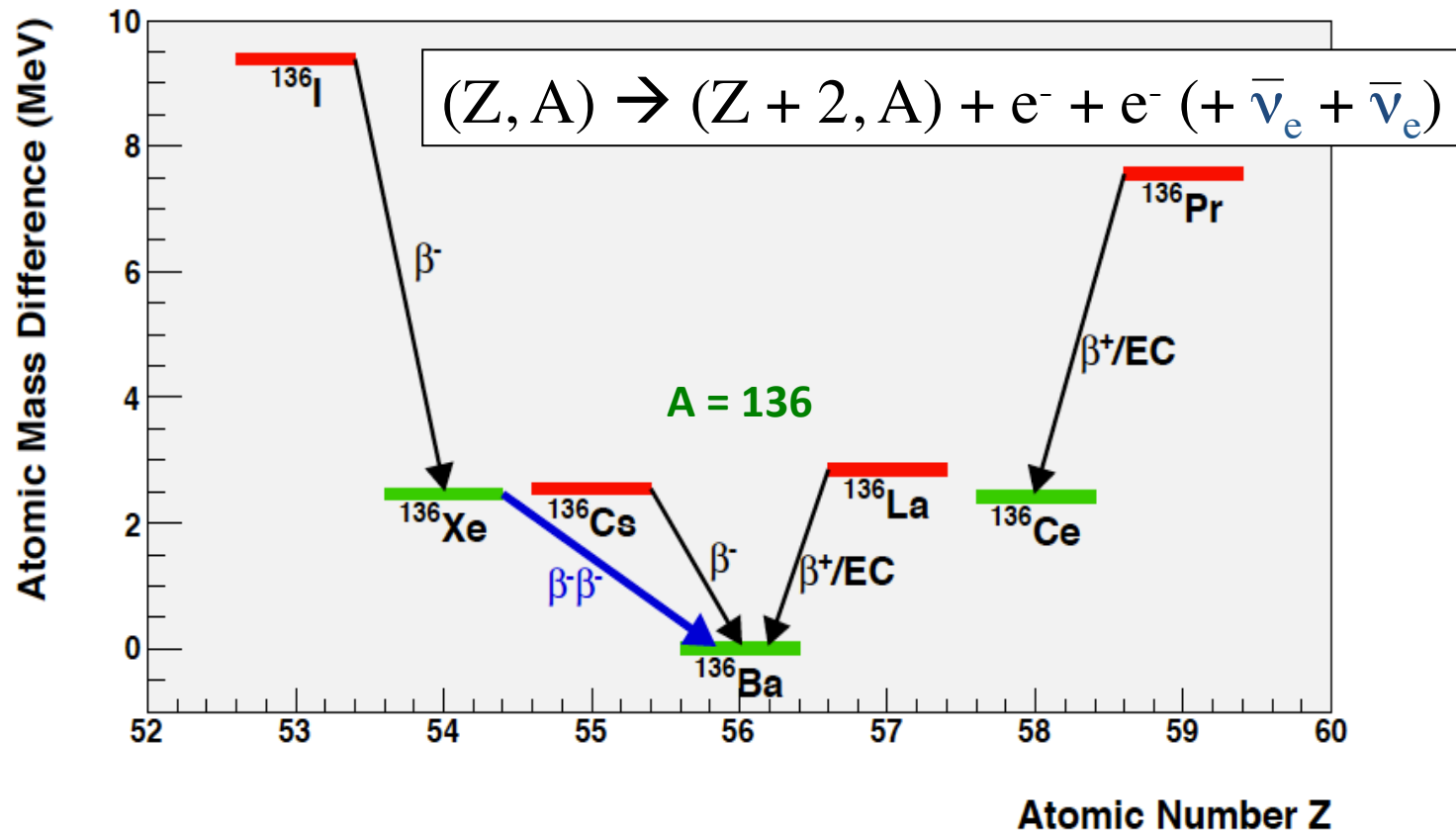
On behalf of the EXO-200 and nEXO collaborations

Drexel University

May 5th, 2015

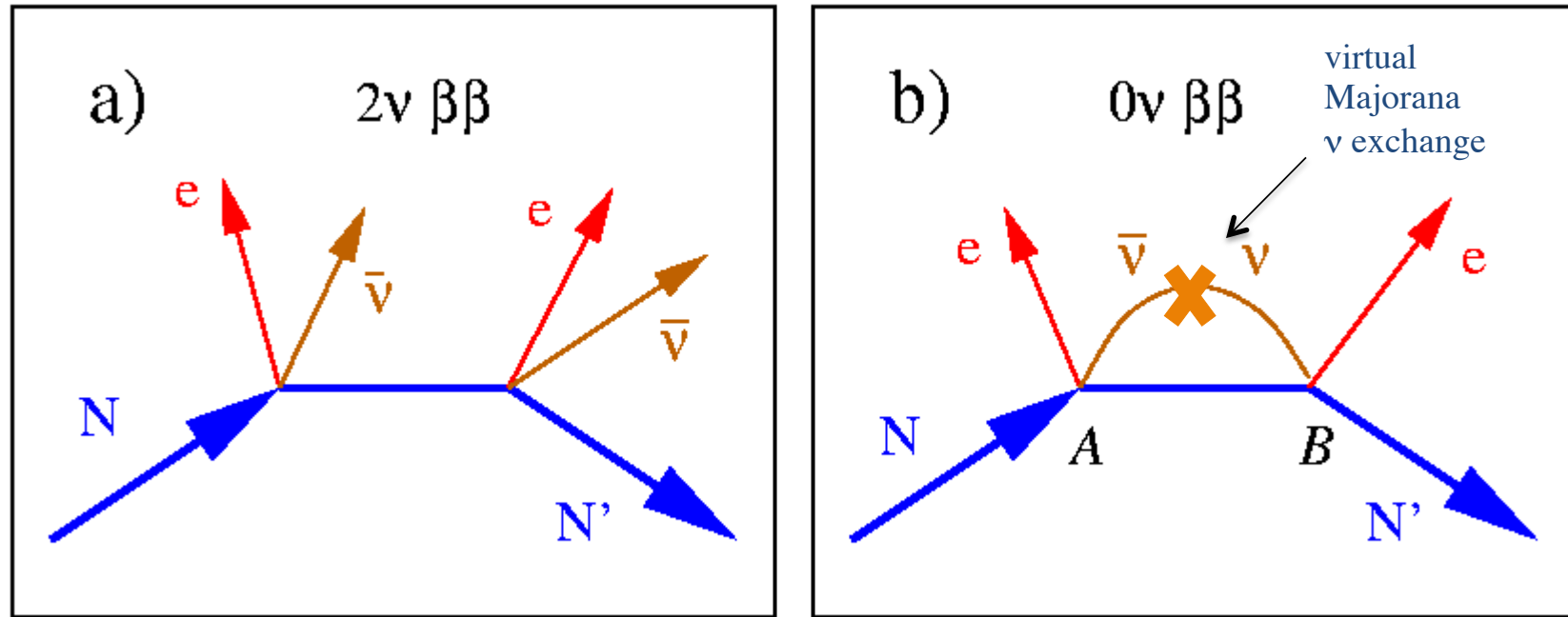
IPA 2015

Double Beta Decay



- If first-order beta decay is forbidden energetically or by spin, second-order double beta decay (a weak nuclear process) can be observed
- True for several isotopes such as: Ca-48, Ge-76, Te-130, **Xe-136**

Two Modes of Double Beta Decay



Two neutrino mode:

- Standard model process
- Second order
- $\Delta L = 0$ (lepton number conserved)



Y.-R. Yen

Neutrinoless mode:

- Hypothetical “Beyond the Standard Model” process
- Can only happen if:
 - neutrino has nonzero mass
 - neutrino is its own antiparticle (**Majorana neutrino**)
- Total lepton number violating ($\Delta L = 2$)

Mass Measurement with $\beta\beta0\nu$

- Half-life depends on the effective mass,

May able to answer
the neutrino mass
hierarchy problem

$$m_{\beta\beta} = \left| \sum_{i=1}^3 m_i U_{ei}^2 \right|$$

mass eigenvalues

mixing matrix
(with phases)

$$\frac{1}{t_{1/2}^{0\nu}} = G^{0\nu} |M^{0\nu}|^2 m_{\beta\beta}^2$$

$\beta\beta0\nu$ Half-life

To be measured

Phase Space

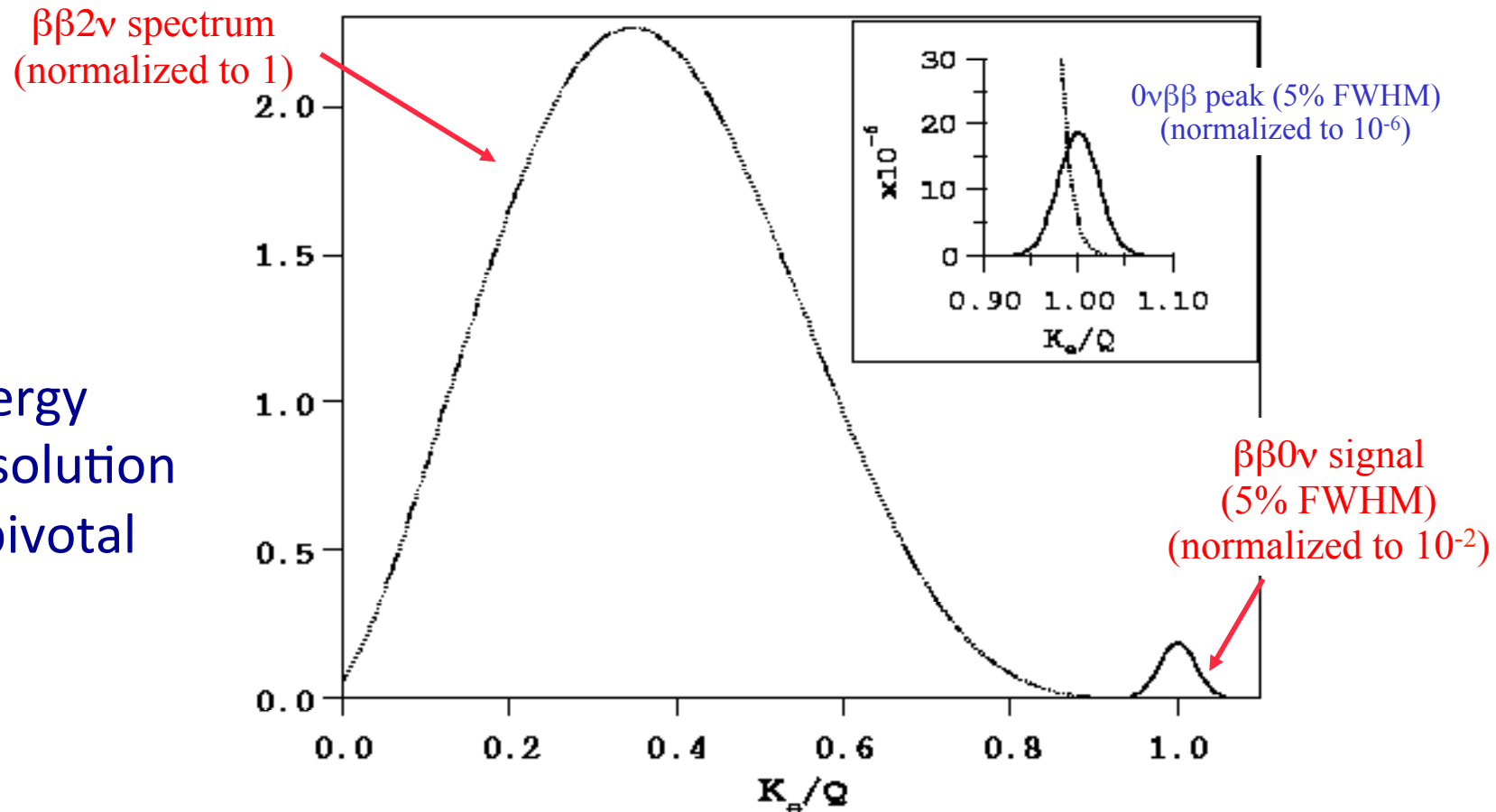
Calculable with
high accuracy

Nuclear Matrix Element

Model dependent (largest
source of uncertainty)

$\beta\beta0\nu$ signature: a peak in the $\beta\beta$ energy spectrum

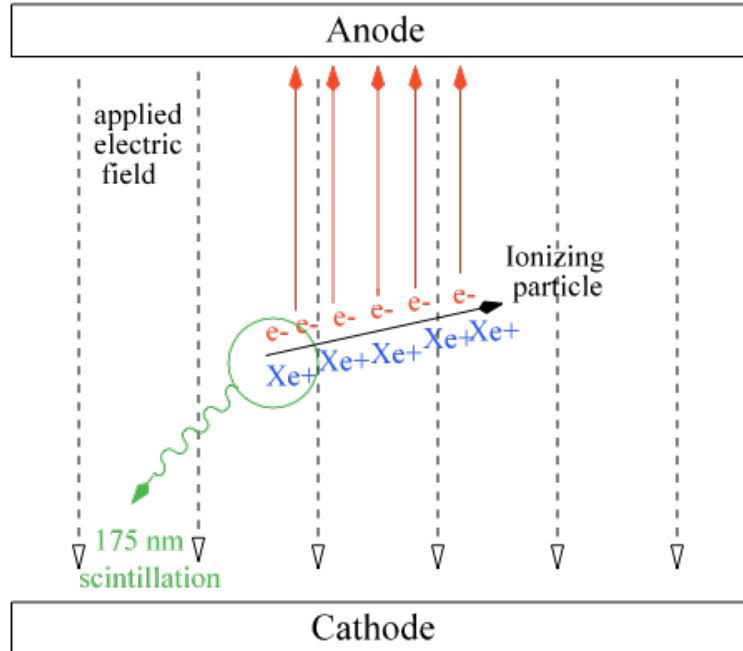
Energy
Resolution
is pivotal



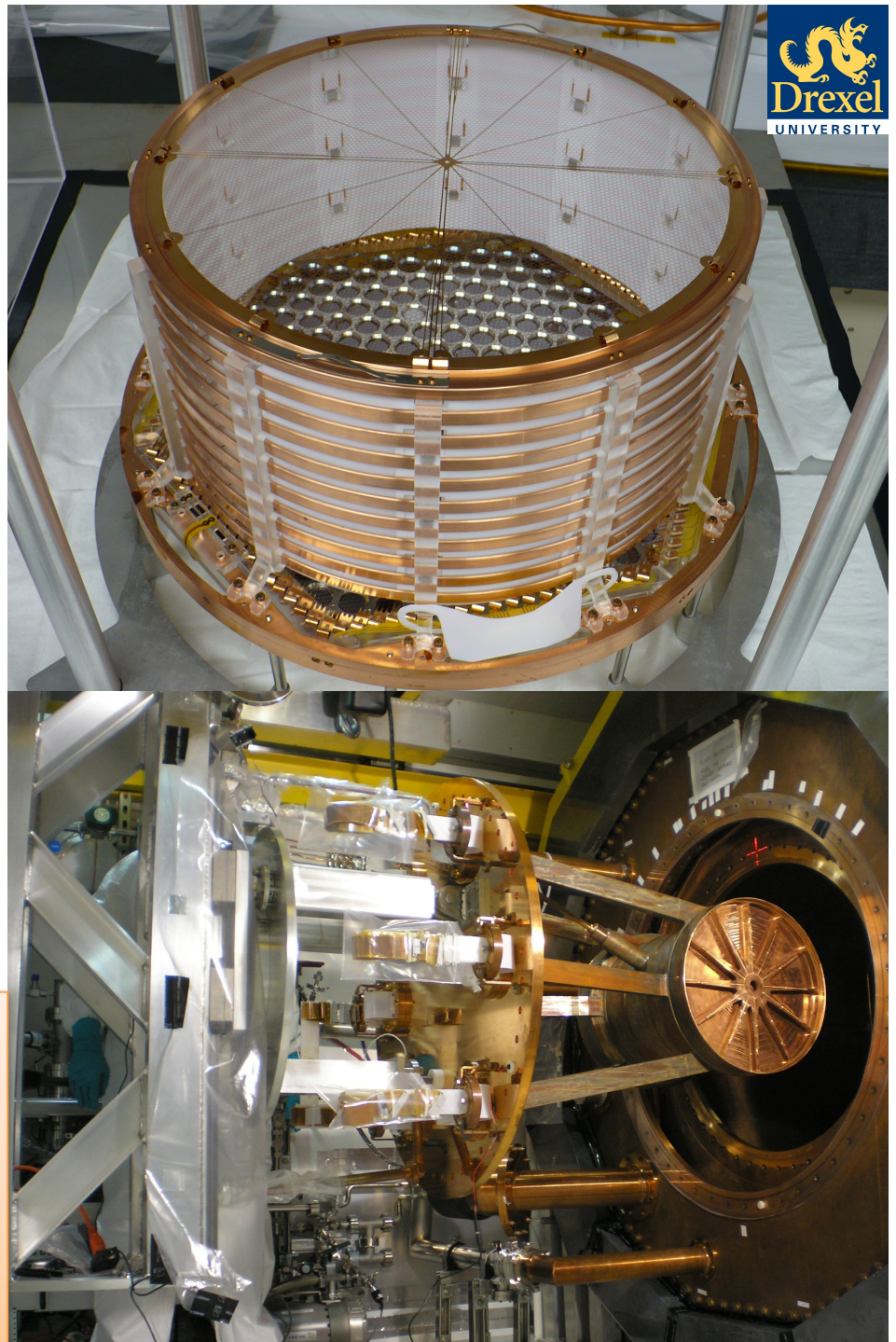


EXO-200

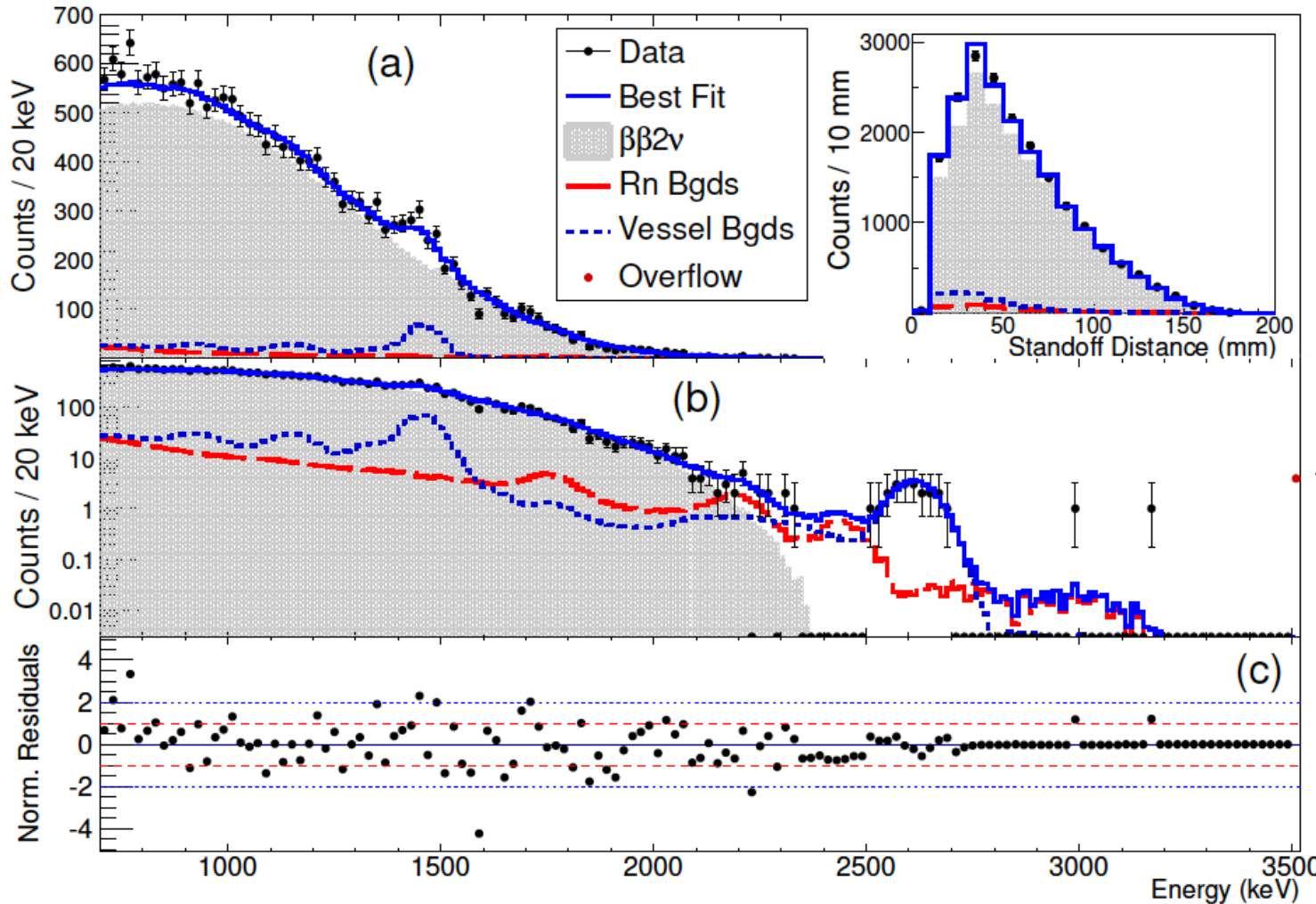
Liquid Xe Time Projection Chamber



~110 kg active mass Xe enriched to 80% in ^{136}Xe , ultralow background construction
Readout plane is made up of LAAPDs (scintillation) + crossed wire grid (ionization)
Achieve electron lifetime in liquid xenon $\tau_e > 2 \text{ ms}$
Began operating with enriched Xe at the Waste Isolation Pilot Plant (WIPP) in May 2011



$2\nu\beta\beta$ precision measurement



$2\nu\beta\beta$ signal to background ratio:
11: 1

Inner 40% fiducial volume signal to background ratio:
19: 1

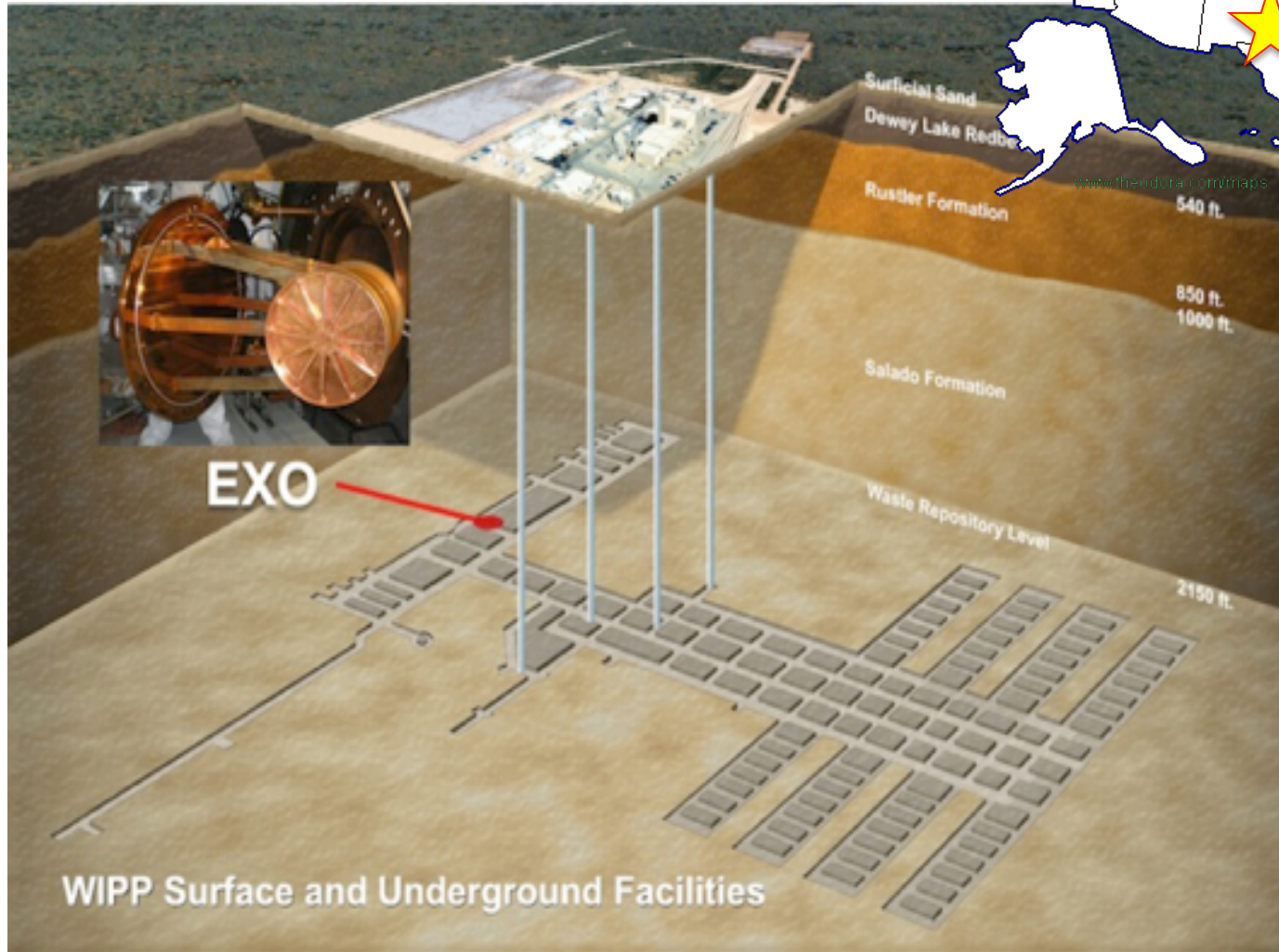
Most precise measurement of the $2\nu\beta\beta$ half-life

$$T_{1/2}^{2\nu\beta\beta} = 2.165 \pm 0.016(\text{stat}) \pm 0.059(\text{sys}) \times 10^{21} \text{ yr}$$

[PRC 89, 015502 (2014)]

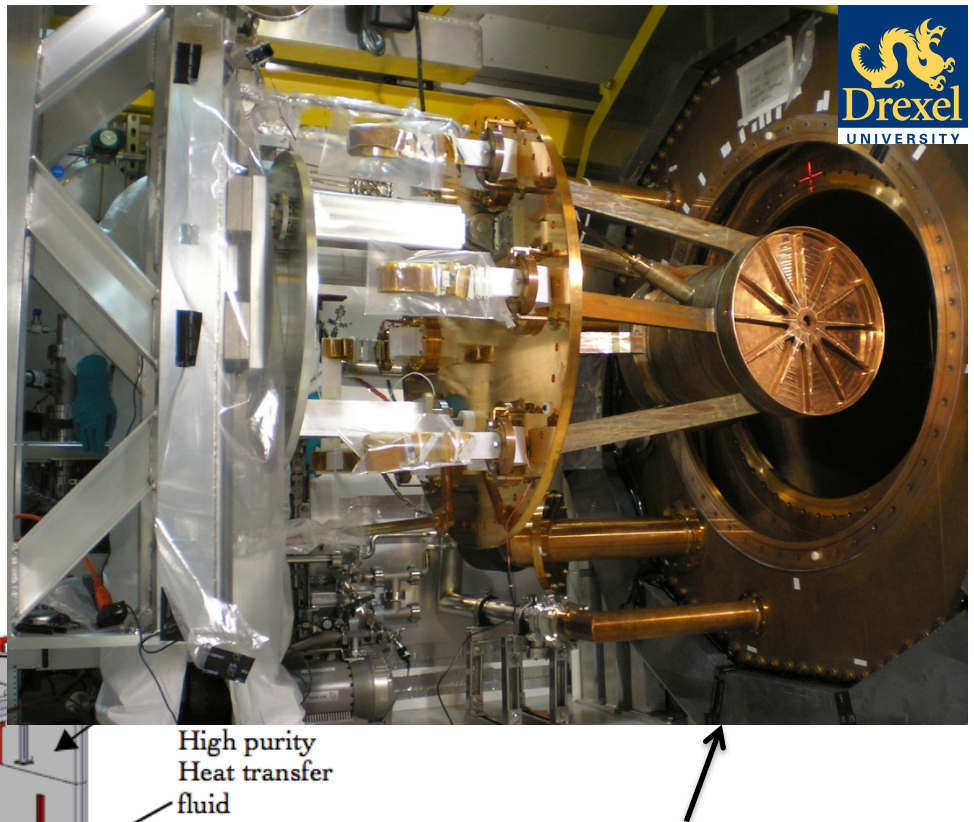
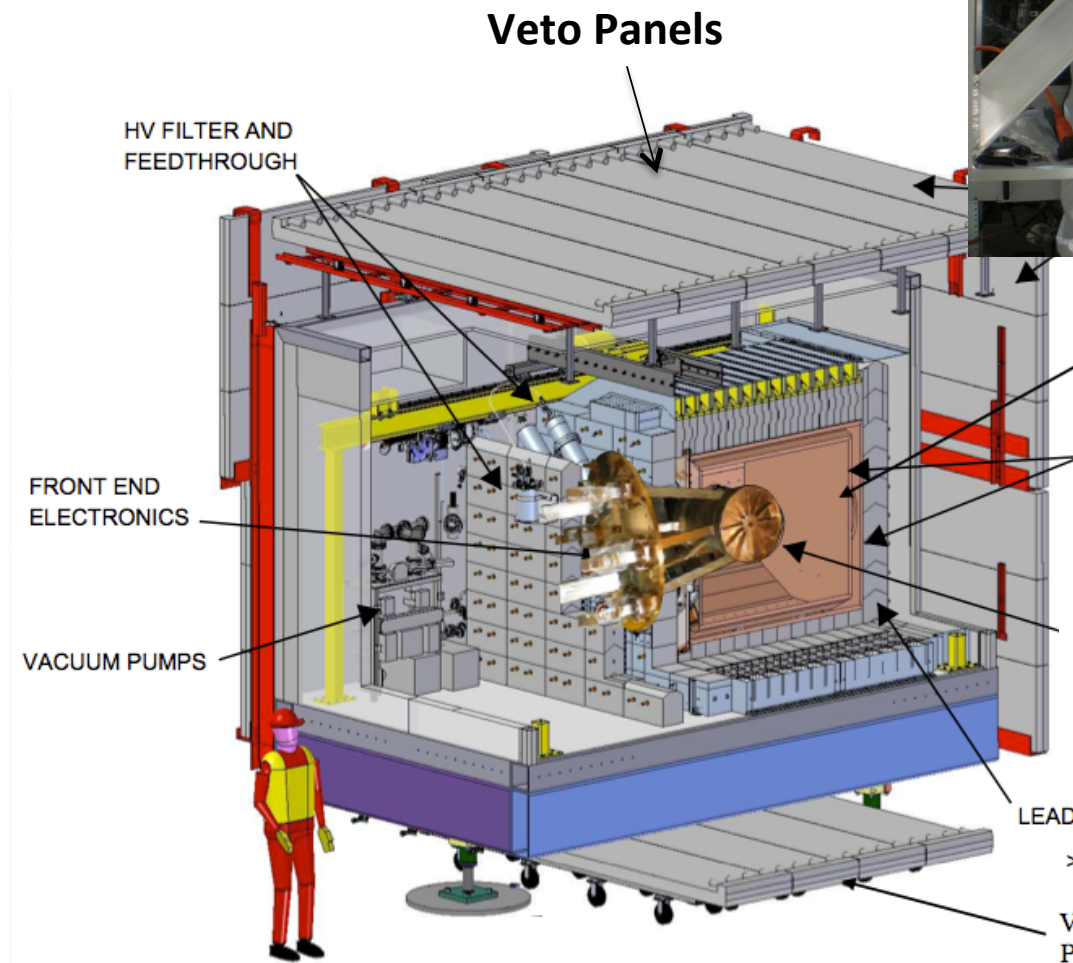


Underground Detector Site



- Waste Isolation Pilot Plant in New Mexico, USA
- Overburden of 1585 meters water equivalent
- low salt radioactivity

Active and Passive Shielding



High purity
Heat transfer
fluid
HFE7000
 > 50 cm
DOUBLE-WALLED
CRYOSTAT
25 mm ea

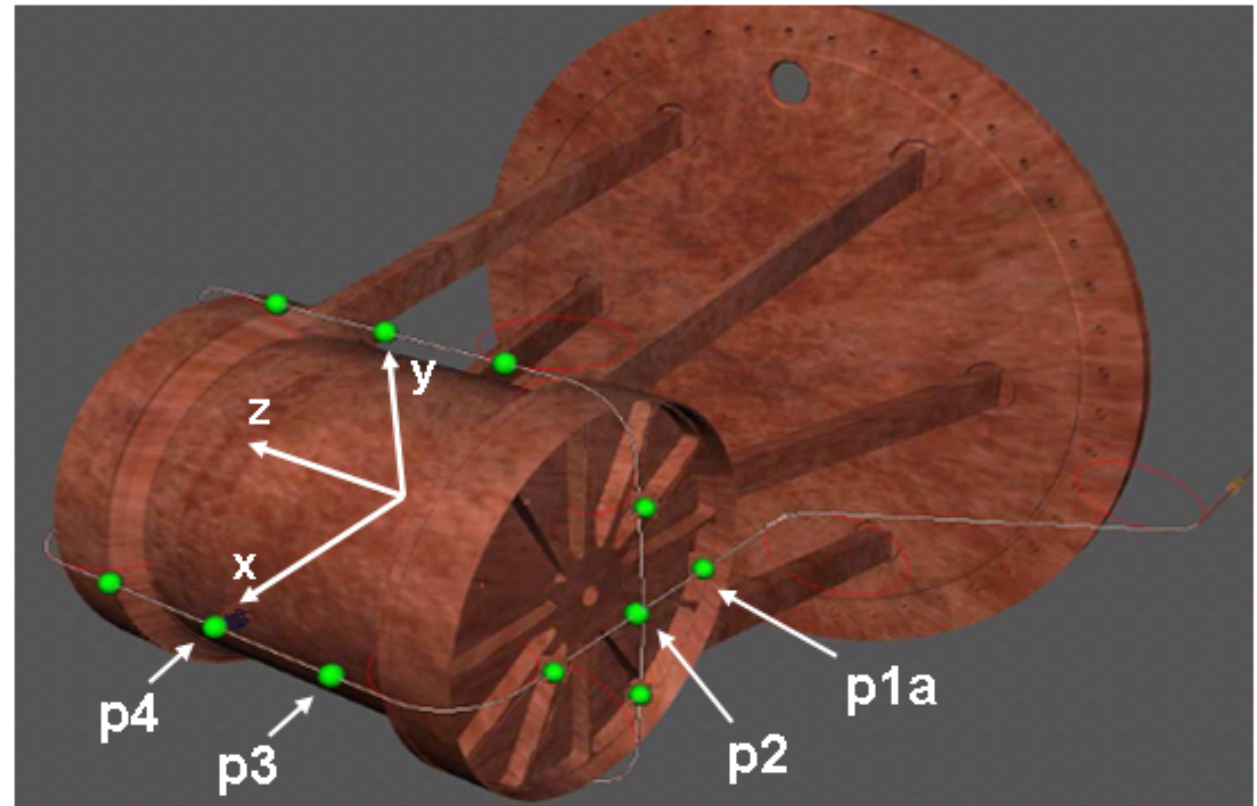
LXe Vessel
1.37 mm

Detector being
installed into the
cryostat system

To minimize the
amount of natural
radioactivity in the
copper “balloon”

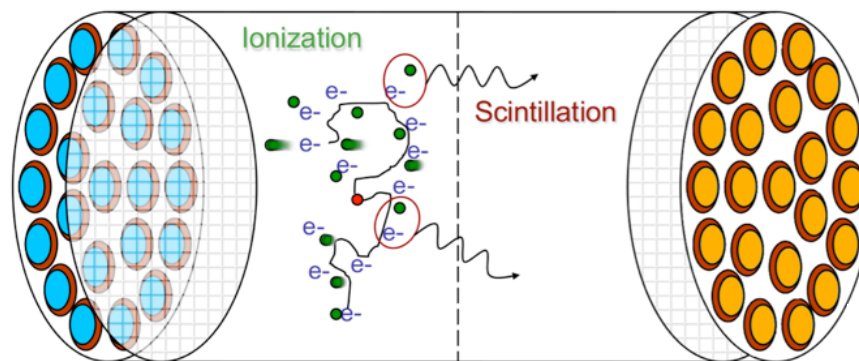
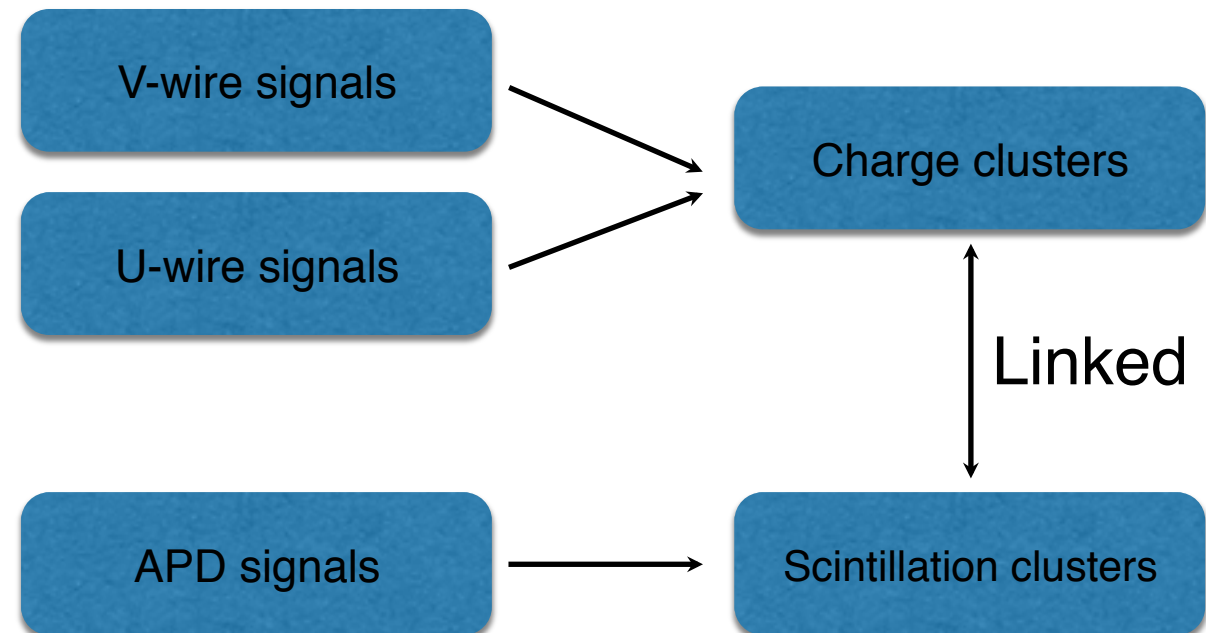
Calibration System

- Periodic campaigns with ^{228}Th , ^{60}Co , and ^{137}Cs , ^{226}Ra
- Main calibration is done with 2615 keV gamma line from ^{228}Th source.



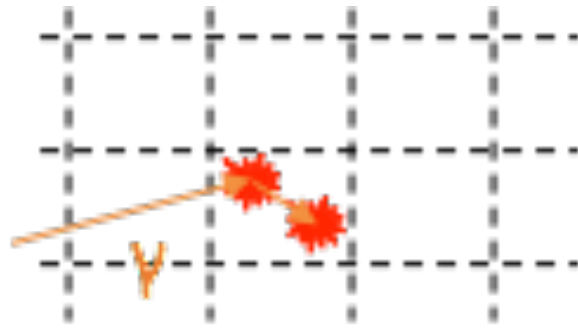
Event reconstruction

1. Event position
2. Event multiplicity
3. Energy measurement

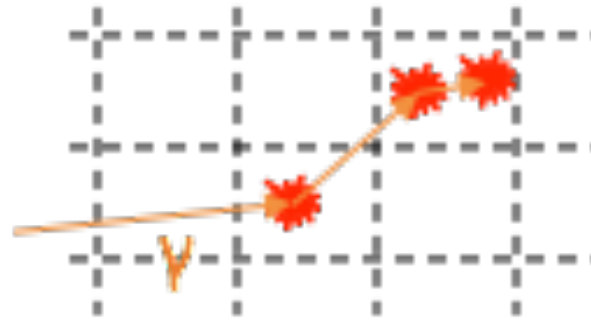


Position and multiplicity reconstruction

Allows for background measurement and reduction



Single-Site (SS) event
(1 charge cluster)



Multi-Site (MS) event
(>1 charge cluster)

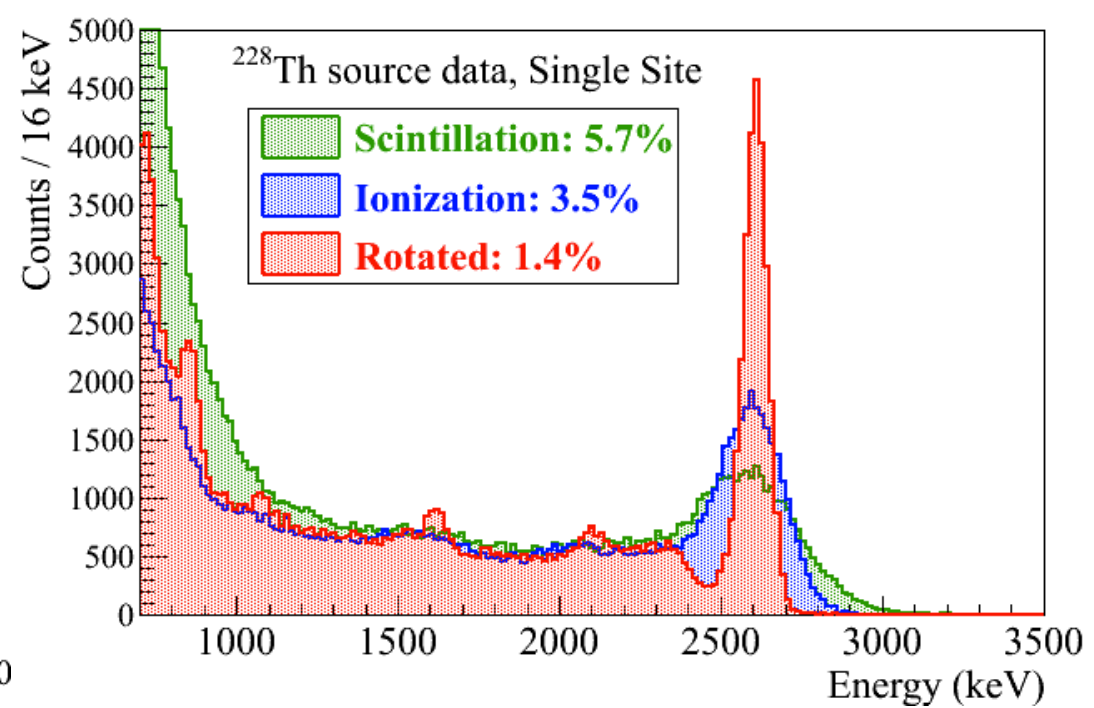
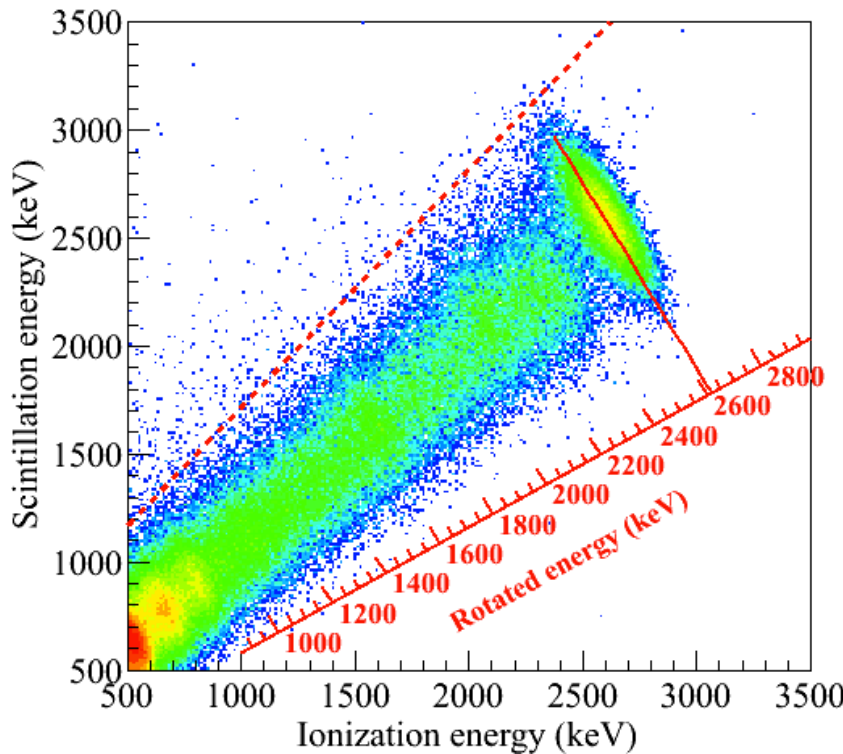
$0\nu\beta\beta$: ~90% SS

γ -rays: ~30% SS at $0\nu\beta\beta$ Q-value

Total error in fiducial volume from position reconstruction: 1.73%

Energy measurement

Anti-correlation of charge and light



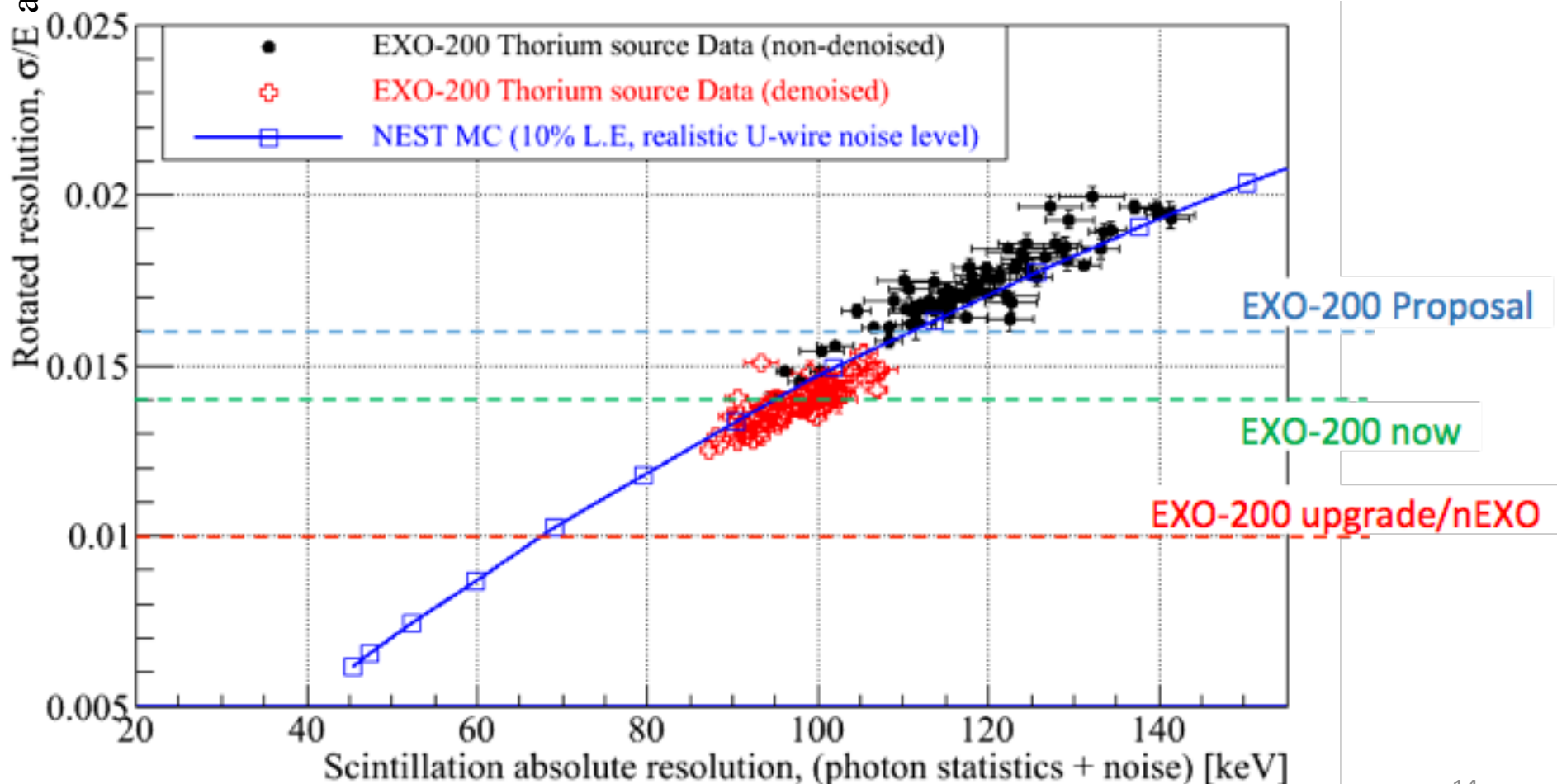
- Rotation angle determined weekly using ^{228}Th source data, defined as angle which gives best rotated resolution
- Energy resolution is dominated by APD noise

APD Denoising

Problem: Resolution is dependent on the time-varying correlated noise of the APDs

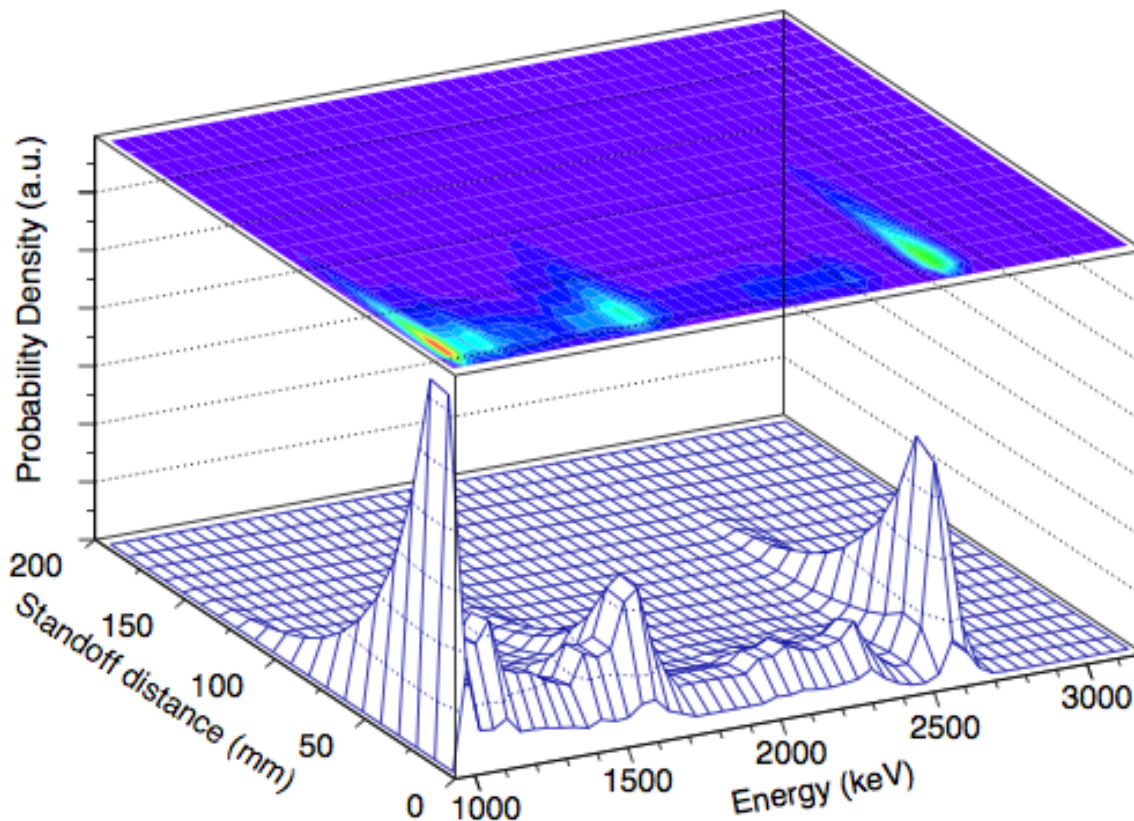
Software solution (current): Find the optimum combination of APD signals *per event*, given position and noise

Hardware solution (future): Planned upgrade of APD readout electronics to reduce noise



Resolution curve from simulation using NEST: <http://nest.physics.ucdavis.edu/>

Extracting physics results



Single site ^{232}Th Probability Density Function in copper vessel

- Variables
 - Energy
 - Position (standoff distance)
- Multiplicity
 - SS
 - MS

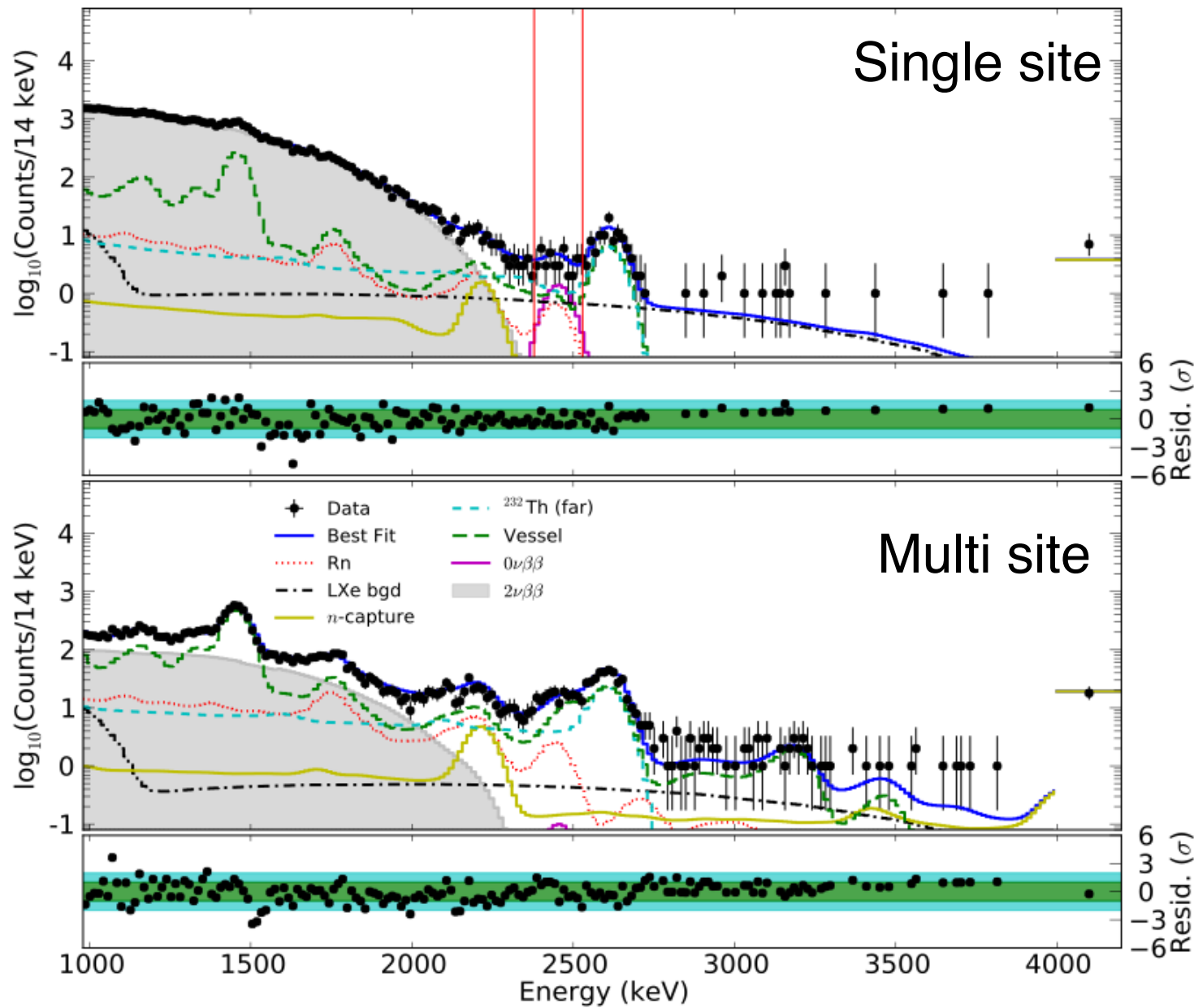
Standoff Distance

- “Standoff” = closest distance between a charge cluster and detector component
- Gammas will be closer to detector sides, $\beta\beta 0\nu$ will be evenly distributed in detector

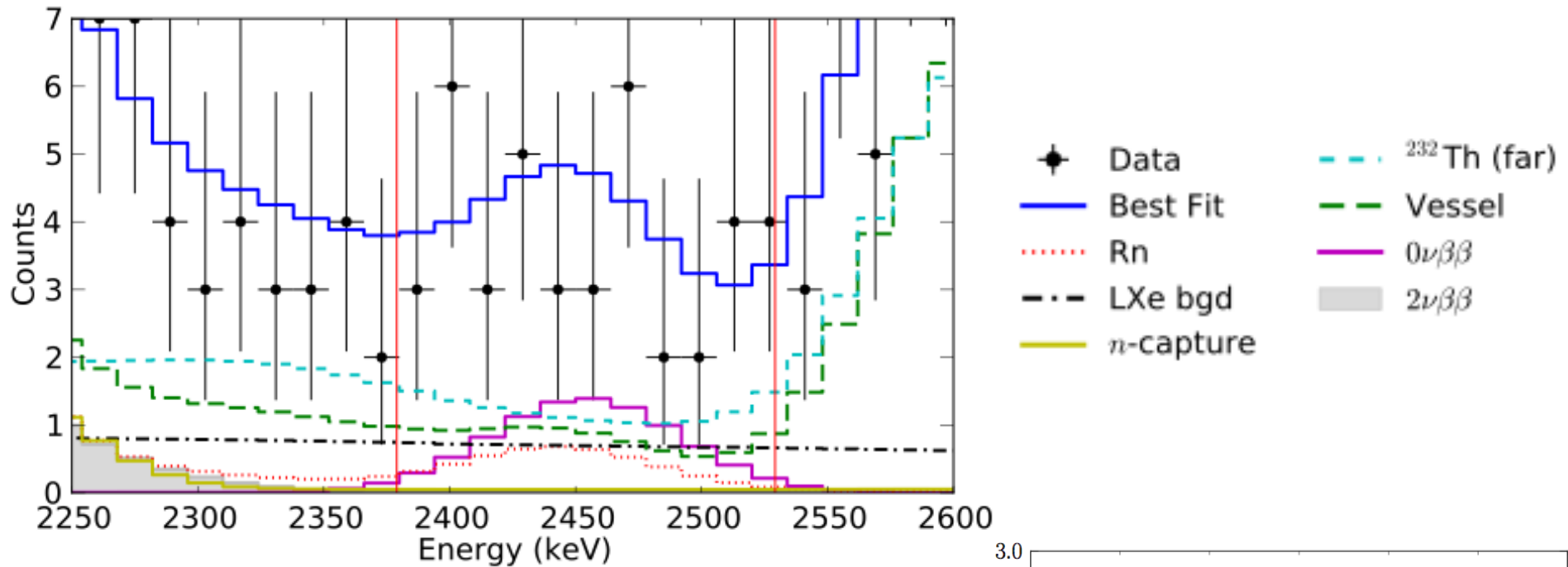
$100 \text{ kg} \cdot \text{yr}$
 $736 \text{ mol} \cdot \text{yr}$ ^{136}Xe exposure

Final Fit

Analysis range:
980 keV to 9800 keV

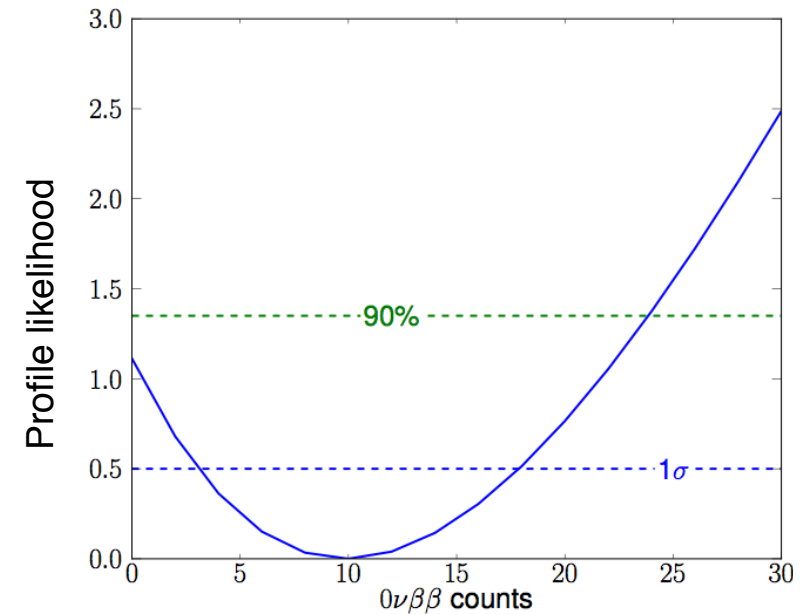


$0\nu\beta\beta$ Search

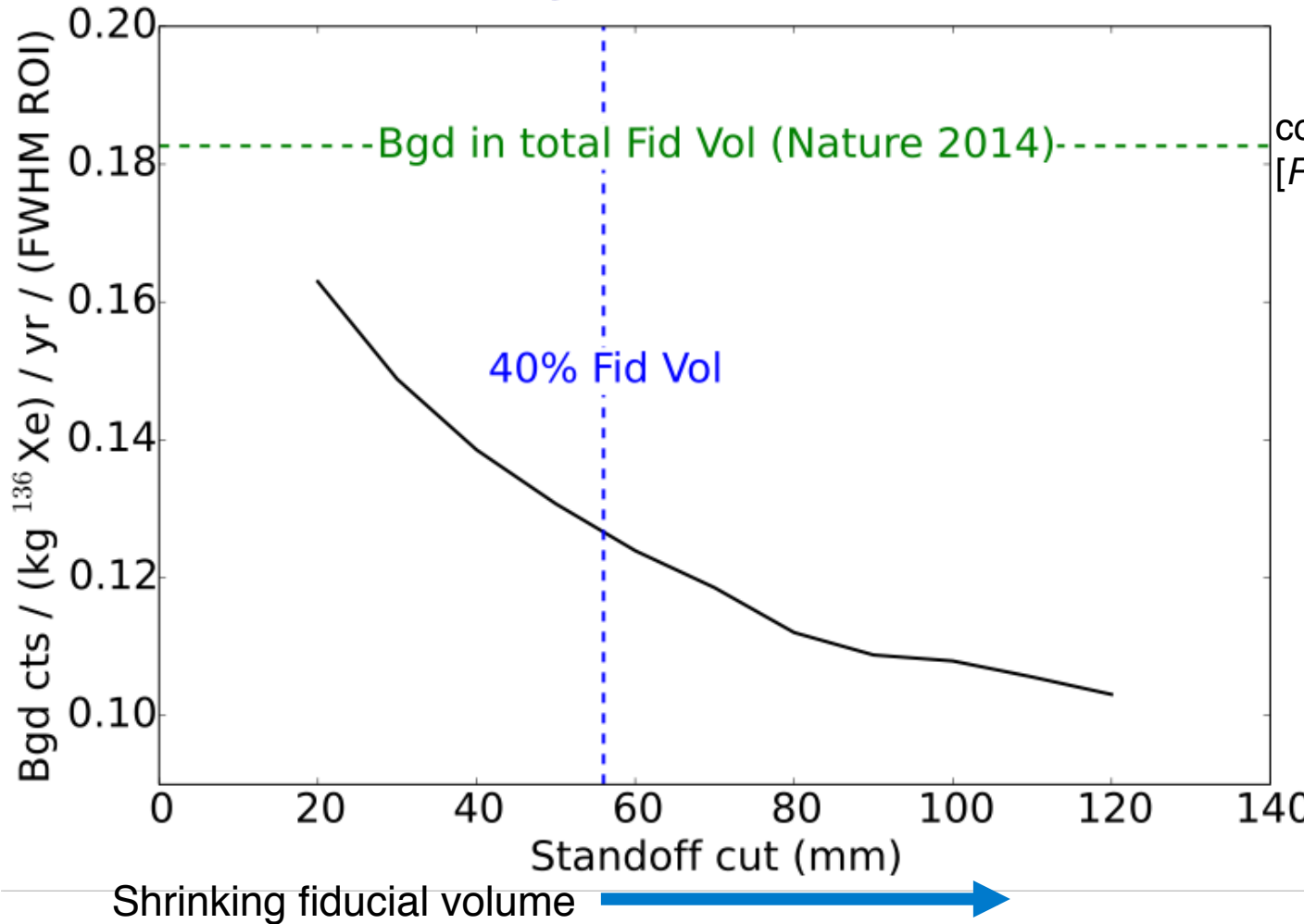


$T_{1/2}^{0\nu\beta\beta} > 1.1 \times 10^{25} \text{ yr}$
 $\langle m_{\beta\beta} \rangle < 190 - 450 \text{ meV}$
(90% C.L.)

[Nature 510, 229 (2014)]



Backgrounds in the ROI



consistent with previous result
[PRL 109, 032505 (2012)]

39 counts in
 $\pm 2\sigma$ ROI

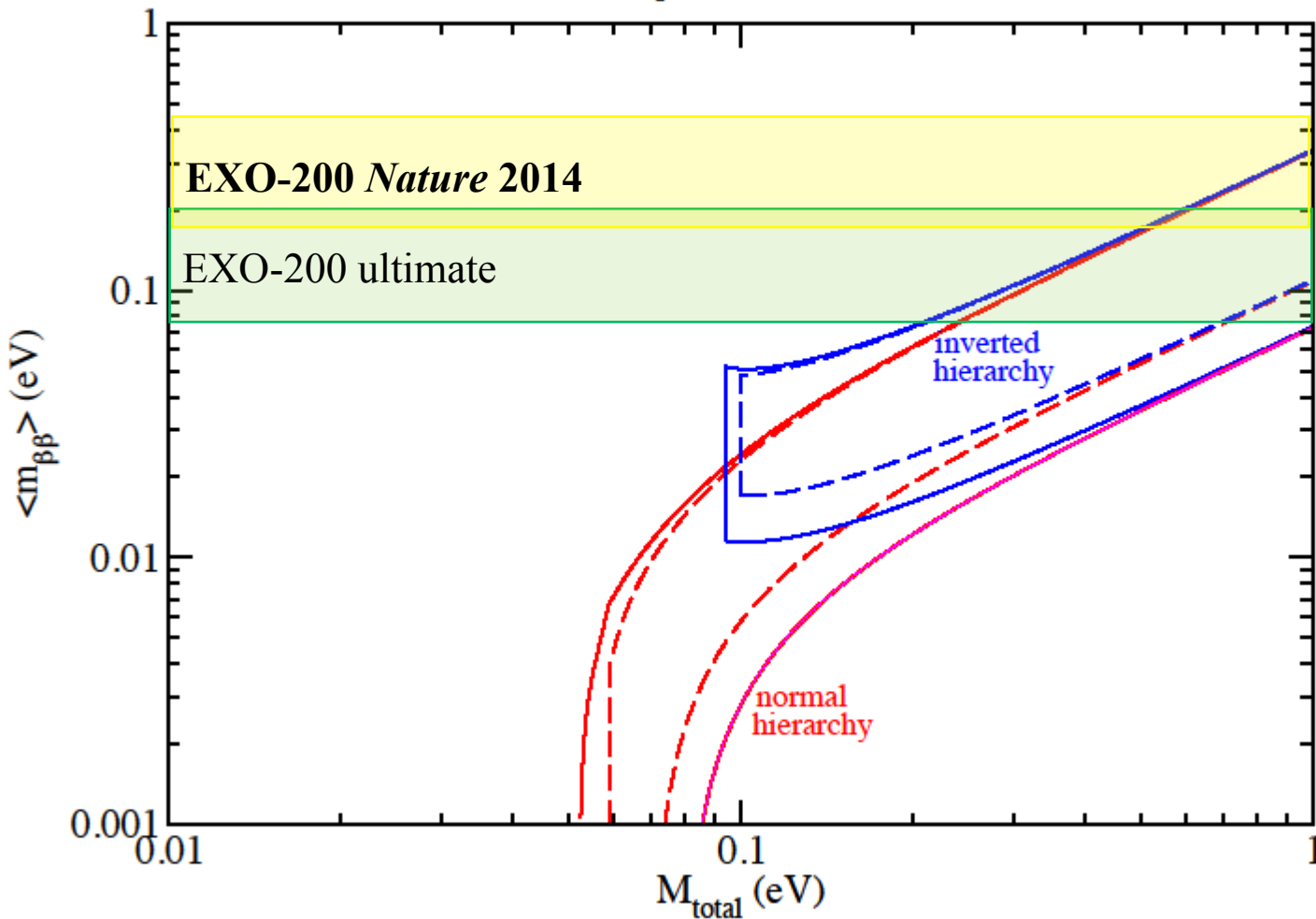
Backgrounds in $\pm 2\sigma$ R.O.I.	
Th-228 chain	16.0
U-232 chain	8.1
Xe-137	7.0
Total	31.1 ± 3.8

30% reduction of background index in inner 40% fiducial volume

Sensitivity outlook

Effective Majorana mass vs. M_{total}

For the mean values of oscillation parameters (dashed) and for the 3σ errors (full)



EXO-200 current sensitivity (90%CL):
 1.9×10^{25} yr

EXO-200 ultimate sensitivity (90%CL):
2 years additional livetime with Rn removal

Majoron modes

Alternatives for Modeling Neutrinoless Double Beta Decay

L_e	A New Scalar:	$\beta\beta_{0\nu}$	Dominant Scalar Decay	Spectral Index
IA	Broken	Does Not Exist	Yes	None
IB	Broken	Is Not a Goldstone Boson	Yes	$\beta\beta_\varphi$
IC	Broken	Is a Goldstone Boson	Yes	$\beta\beta_\varphi$
ID	Broken	Is Not a Goldstone Boson	Yes	$\beta\beta_{\varphi\varphi}$
IE	Broken	Is a Goldstone Boson	Yes	$\beta\beta_{\varphi\varphi}$
IIA	Unbroken	Does Not Exist	No	None
IIB	Unbroken	Is Not a Goldstone Boson ($L_e = -2$)	No	$\beta\beta_\varphi$
IIC	Unbroken	Is Not a Goldstone Boson ($L_e = -1$)	No	$\beta\beta_{\varphi\varphi}$
IID	Unbroken	Is a Goldstone boson ($L_e = -2$)	No	$\beta\beta_\varphi$
IIE	Unbroken	Is a Goldstone boson ($L_e = -1$)	No	$\beta\beta_{\varphi\varphi}$

P. Bamert, C. P. Burgess and R. N. Mohapatra, Nucl. Phys. B 449, 25 (1995) [hep-ph/9412365].

Majorons are Goldstone boson that comes from the spontaneous symmetry breaking (due to a “Mexican Hat” potential of B-L).

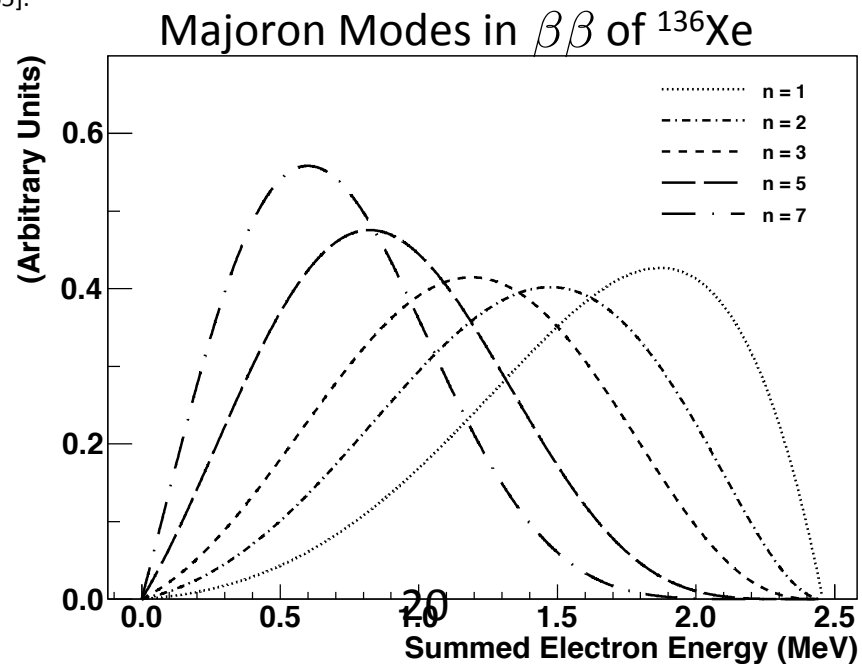


Happy Cinco de Mayo!

Y.-R. Yen

IPA 2015

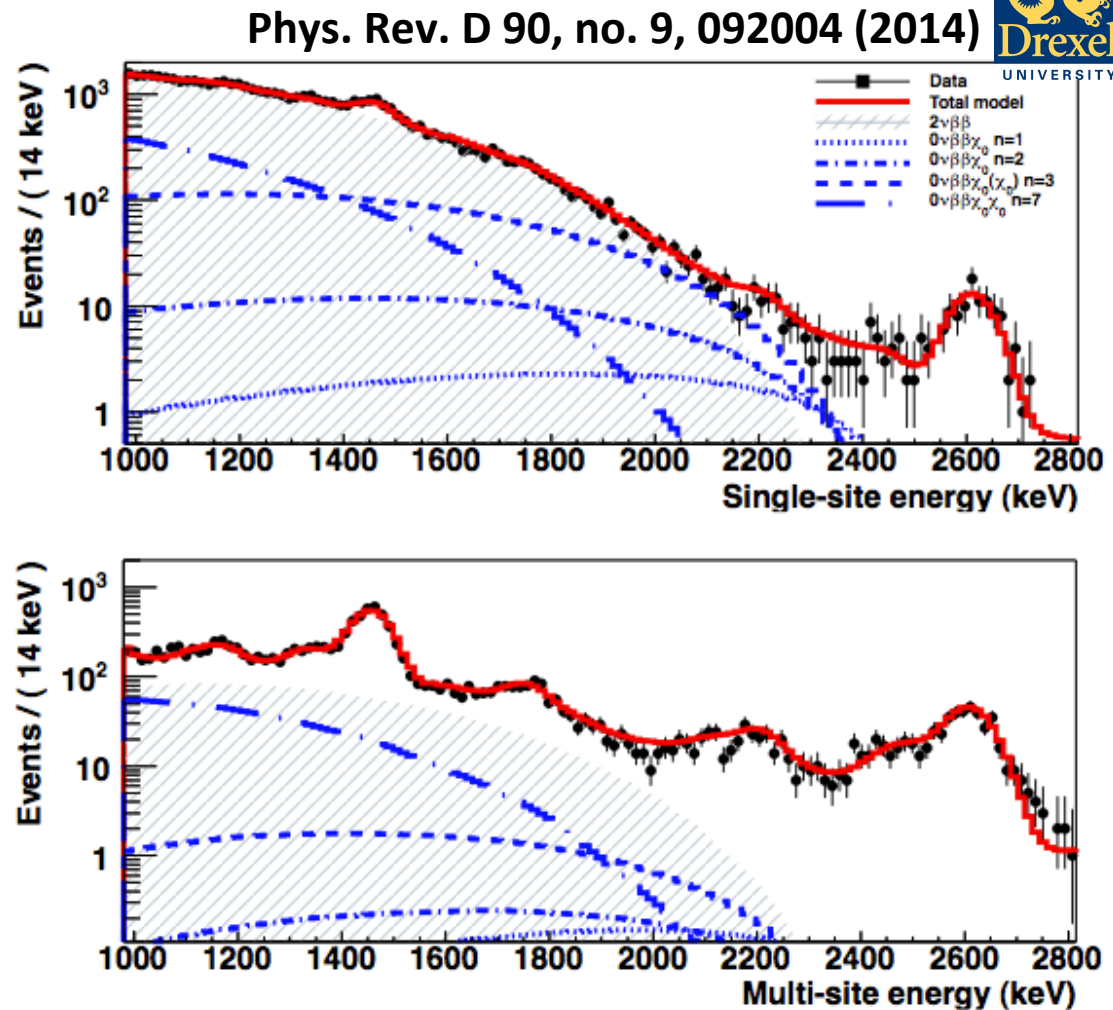
- Alternative theories of $0\nu\beta\beta$ exist: Instead of emitting only electrons, perhaps 1 or 2 new scalar bosons are emitted (Majorons)
- Shape of $\beta\beta$ changes by a spectral index



Majoron Mode Search Result

*Data fit for each Majoron mode separately

*Background shown is for fit to n=1 mode



Decay mode	Spectral index, n	Model types	$T_{1/2}$, yr	$ \langle g_{ee}^M \rangle $
$0\nu\beta\beta\chi_0$	1	IB, IC, IIB “Bulk”	$>1.2 \cdot 10^{24}$	$<(0.8-1.7) \cdot 10^{-5}$
$0\nu\beta\beta\chi_0$	2	ID, IE, IID	$>2.5 \cdot 10^{23}$	—
$0\nu\beta\beta\chi_0\chi_0$	3	IIC, IIF	$>2.7 \cdot 10^{22}$	$<(0.6-5.5)$
$0\nu\beta\beta\chi_0$	3	IIE	$>2.7 \cdot 10^{22}$	<0.06
$0\nu\beta\beta\chi_0\chi_0$	7		$>6.1 \cdot 10^{21}$	$<(0.5-4.7)$



Current EXO-200 Status



- WIPP events:
 - Feb. 5 2014 – Fire in WIPP underground
 - Feb. 14 2014 – Airborne radiological event
- EXO-200 Status:
 - In late Feb. 2014, with remote system access, Xe was successfully recovered (as designed), followed by controlled warm up of TPC/Cryostat.
 - In Sept. 2014, lost underground power but regained access.
 - Power restored in Feb. 2015
 - Sample salt near the experiment show virtually zero contamination from the radiological event
 - Ongoing cleanup and equipment repair/replacement
- Outlook
 - Cooling and filling LXe TPC in the summer 2015
 - Detector upgrade and data taking in the fall 2015

the two-way BREAKING NEWS FROM NPR

america international economy must reads contact us

america

Official Report: Nuclear Waste Accident Caused By Wrong Cat Litter

MARCH 26, 2015 6:40 PM ET

GEOFF BRUMFIELD



The EXO-200 Collaboration



University of Alabama, Tuscaloosa AL, USA - D. Auty, T. Didberidze, M. Hughes, A. Piepke, R. Tsang

University of Bern, Switzerland - S. Delaquis, R. Gornea, T. Tolba, J-L. Vuilleumier

California Institute of Technology, Pasadena CA, USA - P. Vogel

Carleton University, Ottawa ON, Canada - V. Basque, M. Dunford, K. Graham, C. Hargrove, R. Killick, T. Koffas, C. Licciardi, D. Sinclair

Colorado State University, Fort Collins CO, USA - C. Chambers, A. Craycraft, W. Fairbank, Jr., T. Walton

Drexel University, Philadelphia PA, USA - M.J. Dolinski, J.K. Gaison, Y.H. Lin, E. Smith, Y.-R Yen

Duke University, Durham NC, USA - P.S. Barbeau

IHEP Beijing, People's Republic of China - G. Cao, X. Jiang, L. Wen

University of Illinois, Urbana-Champaign IL, USA - D. Beck, M. Coon, J. Ling, J. Walton, L. Yang

Indiana University, Bloomington IN, USA - J. Albert, S. Daugherty, T. Johnson, L.J. Kaufman, T. O'Conner

University of California, Irvine, Irvine CA, USA - M. Moe

ITEP Moscow, Russia - D. Akimov, I. Alexandrov, V. Belov, A. Burenkov, M. Danilov, A. Dolgolenko, A. Karelina, A. Kovalenko, A. Kuchenkov, V. Stekhanov, O. Zeldovich

Laurentian University, Sudbury ON, Canada - B. Cleveland, A. Der Mesrobian-Kabakian, J. Farine, B. Mong, U. Wichoski

University of Maryland, College Park MD, USA - C. Davis, C. Hall

University of Massachusetts, Amherst MA, USA - J. Abdollahi, S. Johnston, K. Kumar, A. Pocar, D. Shy

IBS Center for Underground Physics, Daejeon, South Korea - D.S. Leonard

SLAC National Accelerator Laboratory, Menlo Park CA, USA - M. Breidenbach, R. Conley, T. Daniels, J. Davis, A. Dragone, K. Fouts, R. Herbst, A. Johnson, K. Nishimura, A. Odian, C.Y. Prescott, A. Rivas, P.C. Rowson, J.J. Russell, K. Skarpaas, M. Swift, A. Waite, M. Wittgen

University of South Dakota, Vermillion SD, USA, - R. MacLellan

Stanford University, Stanford CA, USA - T. Brunner, J. Chaves, R. DeVoe, D. Fudenberg, G. Gratta, M. Jewell, S. Kravitz, D. Moore, I. Ostrovskiy, A. Schubert, K. Twelker, M. Weber

Stony Brook University, SUNY, Stony Brook, NY, USA - K. Kumar, O. Njoya, M. Tarka

Technical University of Munich, Garching, Germany - W. Feldmeier, P. Fierlinger, M. Marino

TRIUMF, Vancouver BC, Canada - J. Dilling, R. Krücken, F. Retière, V. Strickland

The nEXO Collaboration



University of Alabama, Tuscaloosa AL, USA - T. Didberidze, M. Hughes, A. Piepke, R. Tsang

University of Bern, Switzerland - S. Delaquis, R. Gornea, T. Tolba, J-L. Vuilleumier

Brookhaven National Laboratory, Upton NY, USA - M. Chiu, G. De Geronimo, S. Li, V. Radeka, T. Rao, G. Smith, T. Tsang, B. Yu

California Institute of Technology, Pasadena CA, USA - P. Vogel

Carleton University, Ottawa ON, Canada - Y. Baribeau, V. Basque, M. Bowcock, M. Dunford, K. Graham, P. Gravelle, R. Killick, T. Koffas, C. Licciardi, E. Mane, K. McFarlane, R. Schnarr, D. Sinclair

Colorado State University, Fort Collins CO, USA - C. Chambers, A. Craycraft, W. Fairbank, Jr., T. Walton

Drexel University, Philadelphia PA, USA - M.J. Dolinski, Y.H. Lin, E. Smith, Y.-R Yen

Duke University, Durham NC, USA - P.S. Barbeau, G. Swift

University of Erlangen-Nuremberg, Erlangen Center for Astroparticle Physics, Erlangen, Germany - G. Anton, J. Hoessl, T. Michel

IHEP Beijing, People's Republic of China - G. Cao, X. Jiang, H. Li, Z. Ning, X. Sun, N. Wang, W. Wei, L. Wen, W. Wu

University of Illinois, Urbana-Champaign IL, USA - D. Beck, M. Coon, S. Homiller, J. Ling, J. Walton, L. Yang

Indiana University, Bloomington IN, USA - J. Albert, S. Daugherty, T. Johnson, L.J. Kaufman, G. Visser, J. Zettlemoyer

University of California, Irvine, Irvine CA, USA - M. Moe

ITEP Moscow, Russia - D. Akimov, I. Alexandrov, V. Belov, A. Burenkov, M. Danilov, A. Dolgolenko, A. Karelina, A. Kovalenko, A. Kuchenkov, V. Stekhanov, O. Zeldovich

Laurentian University, Sudbury ON, Canada - B. Cleveland, A. Der Mesrobian-Kabakian, J. Farine, B. Mong, U. Wichoski

Lawrence Livermore National Laboratory, Livermore, CA, USA - M. Heffner, A. House, S. Sangiorgio

University of Massachusetts, Amherst MA, USA - J. Dalmasson, S. Johnston, A. Pocar

Oak Ridge National Laboratory, Oak Ridge TN, USA - L. Fabris, D. Hornback, R.J. Newby, K. Ziock

IBS Center for Underground Physics, Daejeon, South Korea - D.S. Leonard

SLAC National Accelerator Laboratory, Menlo Park CA, USA - T. Daniels, K. Fouts, G. Haller, R. Herbst, K. Nishimura, A. Odian, P.C. Rowson, K. Skarpaas

University of South Dakota, Vermillion SD, USA - R. MacLellan

Stanford University, Stanford CA, USA - T. Brunner, J. Chaves, R. DeVoe, D. Fudenberg, G. Gratta, M. Jewell, S. Kravitz, D. Moore, I. Ostrovskiy, A. Schubert, K. Twelker, M. Weber

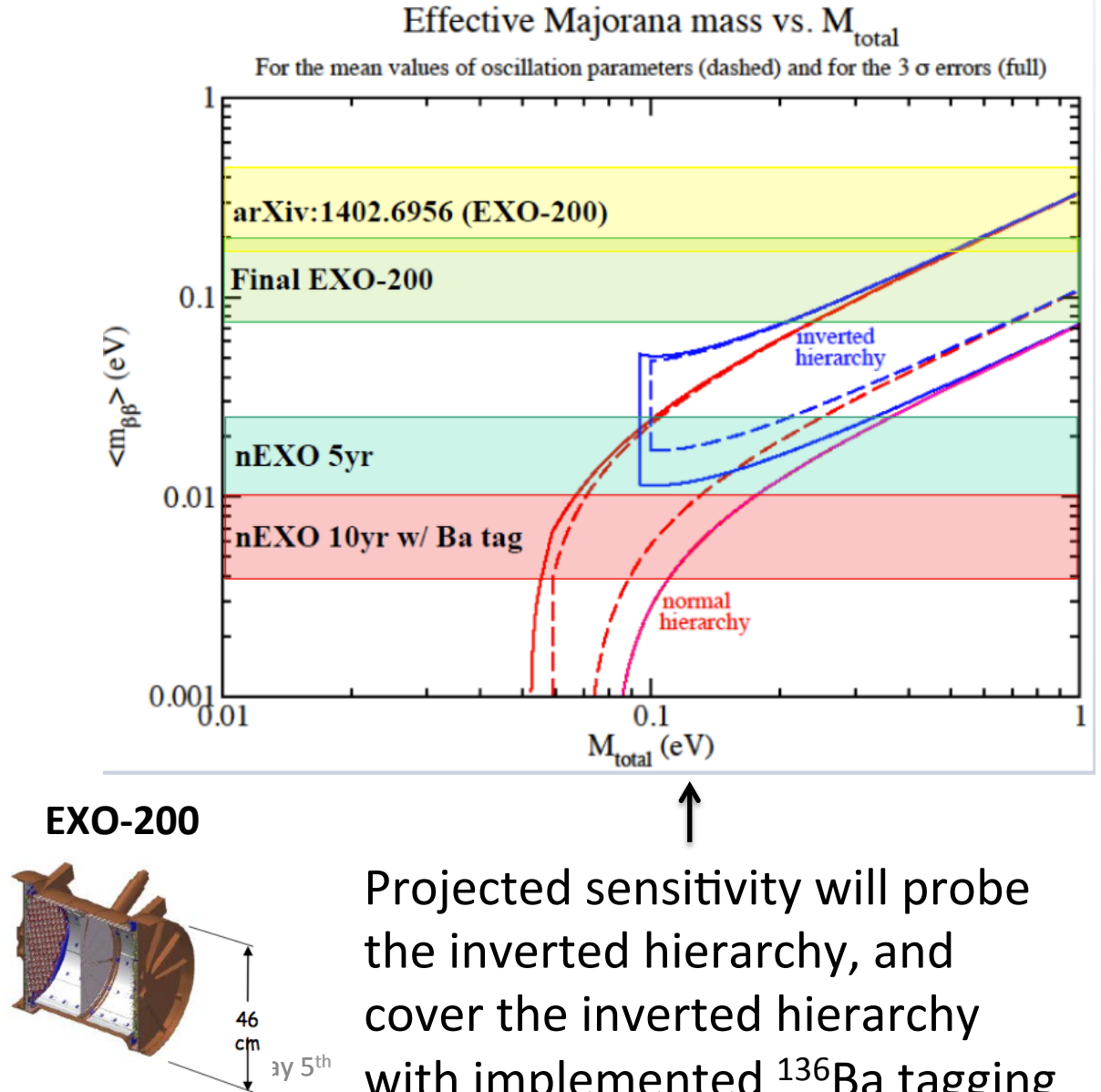
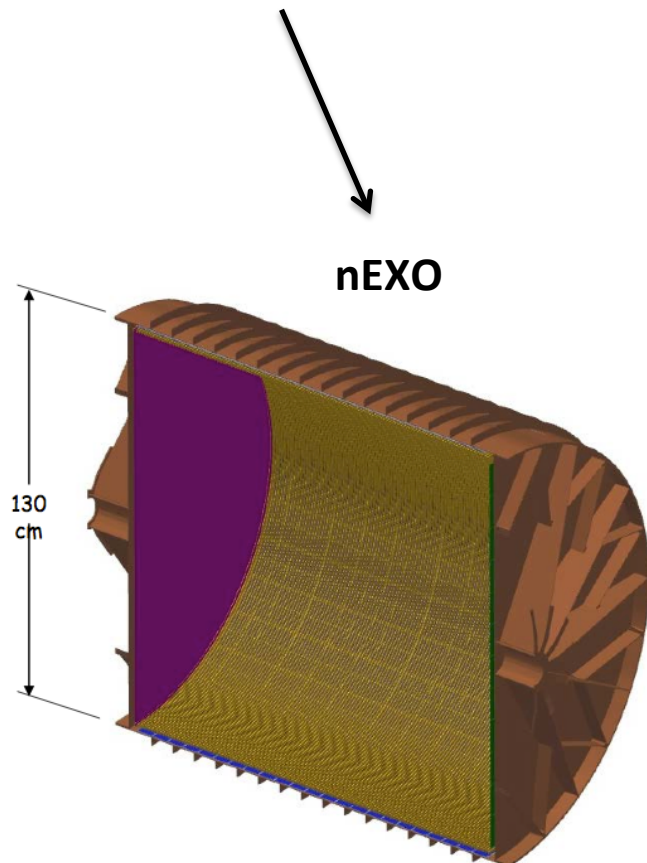
Stony Brook University, SUNY, Stony Brook, NY, USA - K. Kumar, O. Njoya, M. Tarka

Technical University of Munich, Garching, Germany - P. Fierlinger, M. Marino IPA 2015 – May 5th

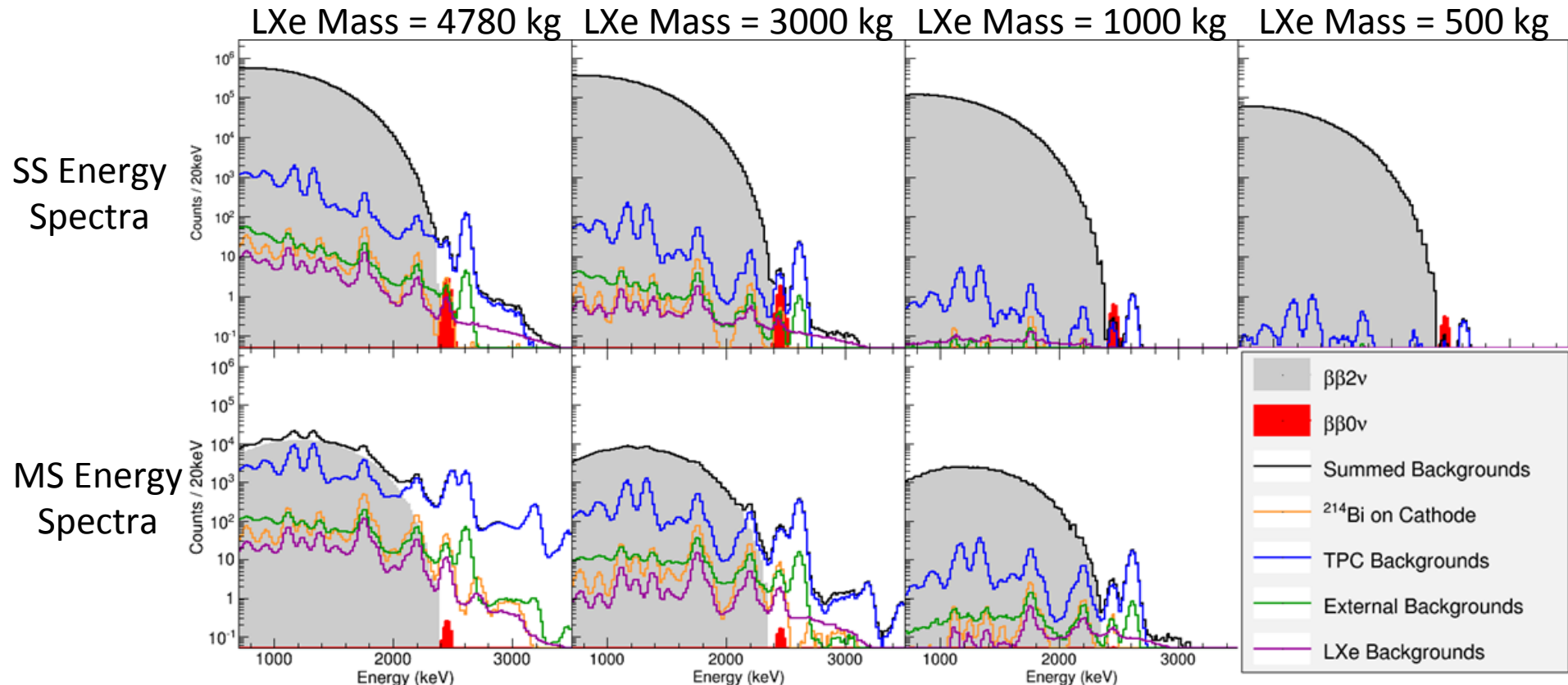
TRIUMF, Vancouver BC, Canada - J. Dilling, P. Gumplinger, R. Krücken, F. Retière, V. Strickland

nEXO (“next EXO”)

A detector 50x the size of EXO-200 is being designed



Backgrounds and Signal

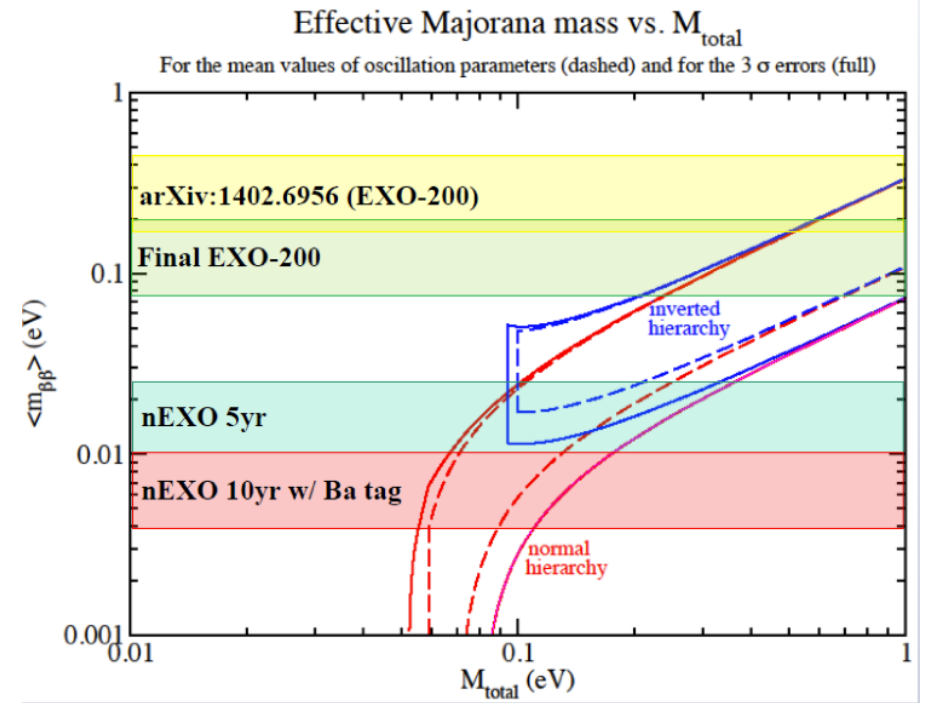


Energy spectra for different LXe masses, with energy discrimination at different positions in the detector without statistical fluctuations, after 5 year exposure.

nEXO sensitivity: $6.6 \cdot 10^{27}$ yr

nEXO vs. EXO-200

Parameter	nEXO	EXO-200
Fiducial mass (kg)	4780	98.5
Enrichment (%)	80-90	80
Data taking time (yr)	5	5
Energy resolution @ $Q_{\beta\beta}$ (keV)	58	88 (58)
Depth (m.w.e)	6010	1500
Background within FWHM of endpoint (events/yr/mol ₁₃₆)	6.1×10^{-4}	0.022 (0.0073)
Background within FWHM of endpoint inner 3000kg (events/yr/mol ₁₃₆)	1.6×10^{-4}	





Summary

- EXO-200 is among the most sensitive $0\nu\beta\beta$ experiments, achieving $100 \text{ kg} \cdot \text{yr}$ exposure of ^{136}Xe . Latest analysis includes substantial improvements in understanding systematics and improving energy resolution.

Sensitivity: $1.9 \times 10^{25} \text{ yr}$

Measurement: $T_{1/2}^{0\nu\beta\beta} > 1.1 \times 10^{25} \text{ yr}$

$\langle m_{\beta\beta} \rangle < 190 - 450 \text{ meV (90\% C.L.)}$

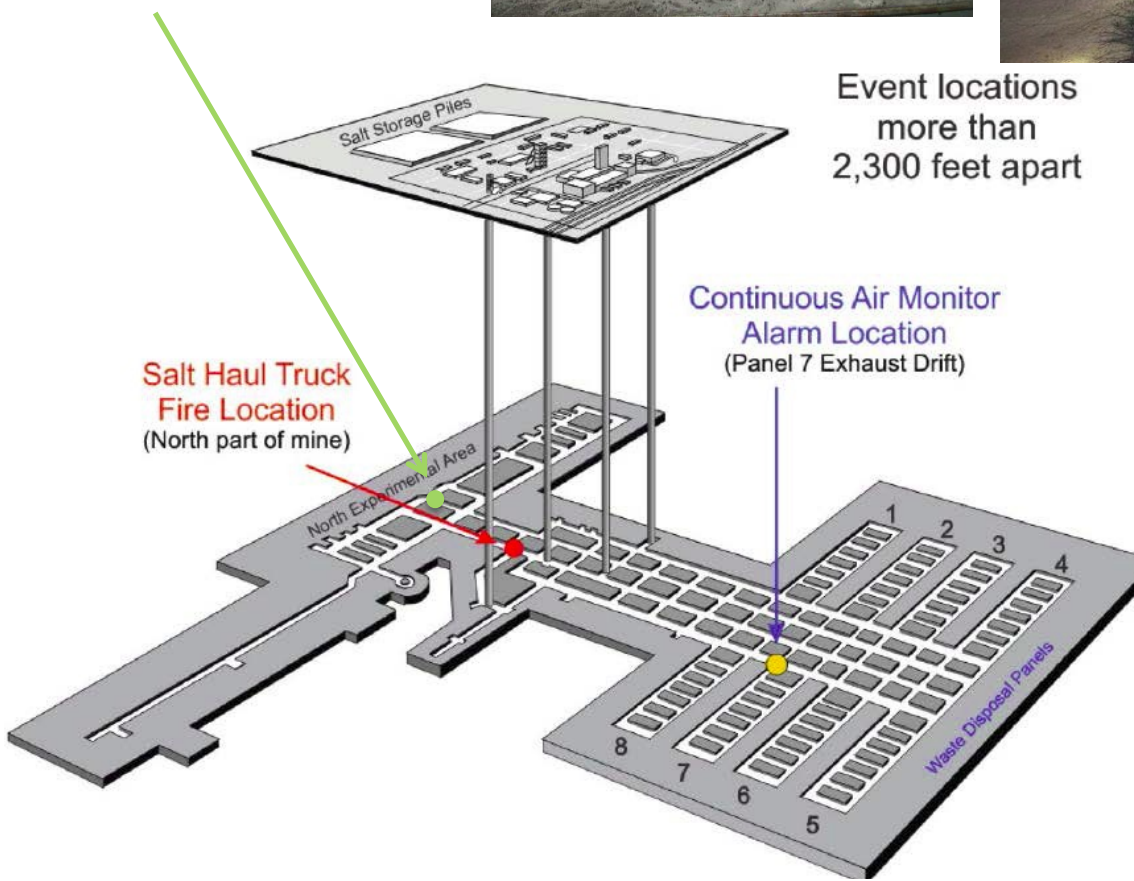
[*Nature* 510, 229 (2014)]

- Majoron limits recently published. Look out for our papers on other exotica searches.
- Data taking has stopped because of WIPP closure, but planned deployment of new electronics and radon removal system should occur in 2015 to achieve optimal EXO-200.
- nEXO plans to take advantage of the scalability of LXe in a next-generation ~5 tonne experiment and build upon the experiences from EXO-200.

EXTRA SLIDES

The future of EXO-200

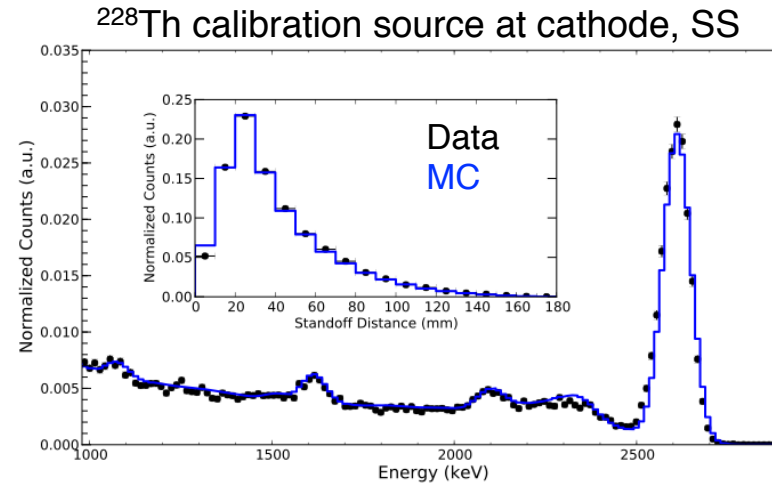
EXO-200 is nearly
4000 feet from the
radiation event



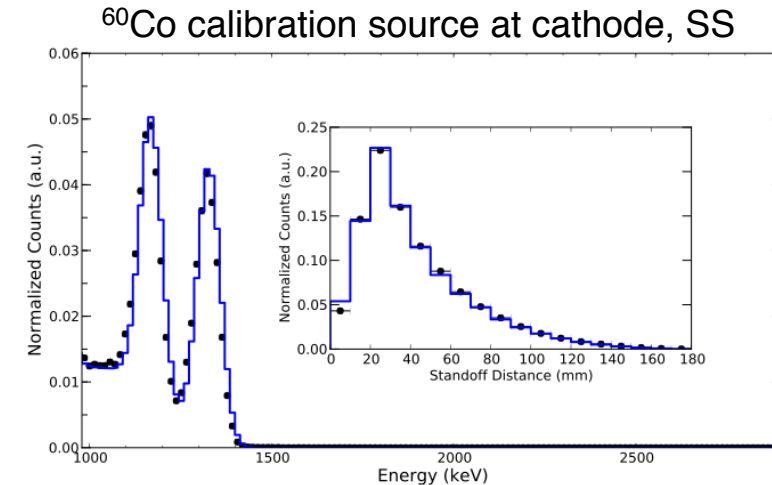
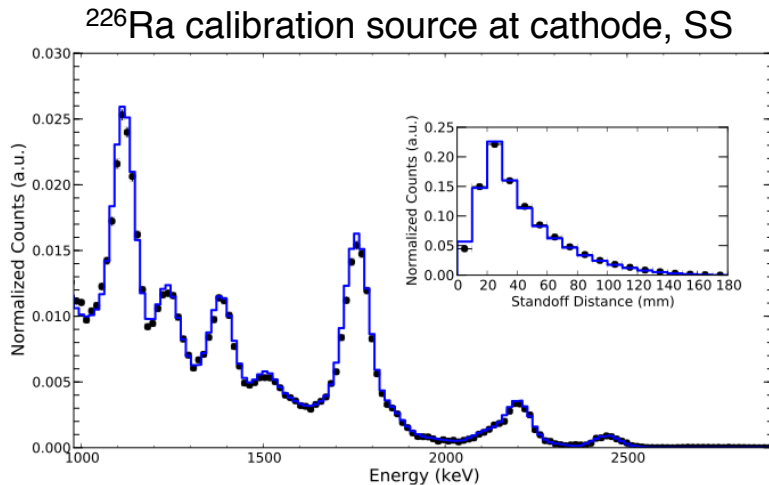
- **Feb. 5 2014:** Fire in WIPP underground
- **Feb. 14, 2014:** Radiation release event
- So far no radioactivity has been measured at EXO-200
- EXO clean up has started
- A restart with new electronics and radon removal system targeted for 2015

Source Shape Agreement

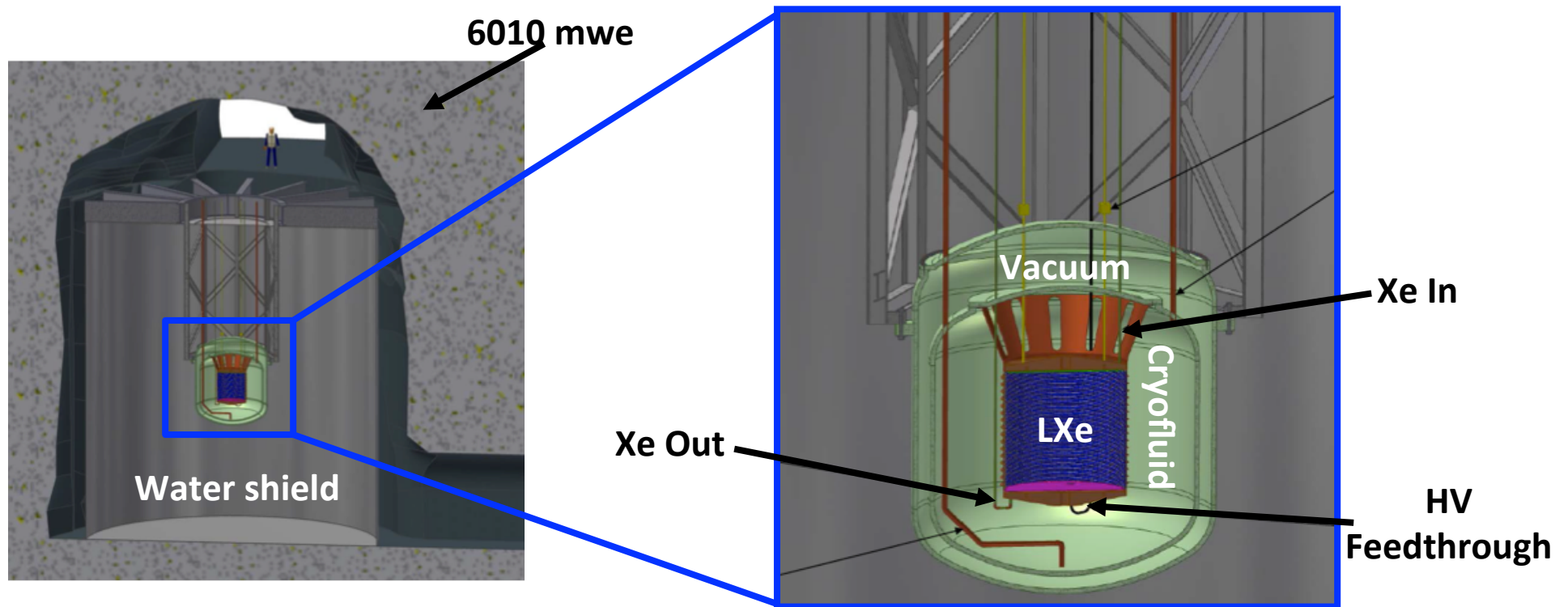
- Monte Carlo simulations accurately reproduce the spectral shapes of the energy and standoff distance distributions we see in data, for our calibration sources
- The most notable shape discrepancy occurs in the first standoff distance bin, where MC is predicting more events than seen in data by $\sim 25\%$
- Residual energy and standoff distance shape discrepancies between data and MC are used to define a systematic error resulting from background PDF shape distortion errors



Energy binning: 14 keV, standoff distance binning: 10 mm



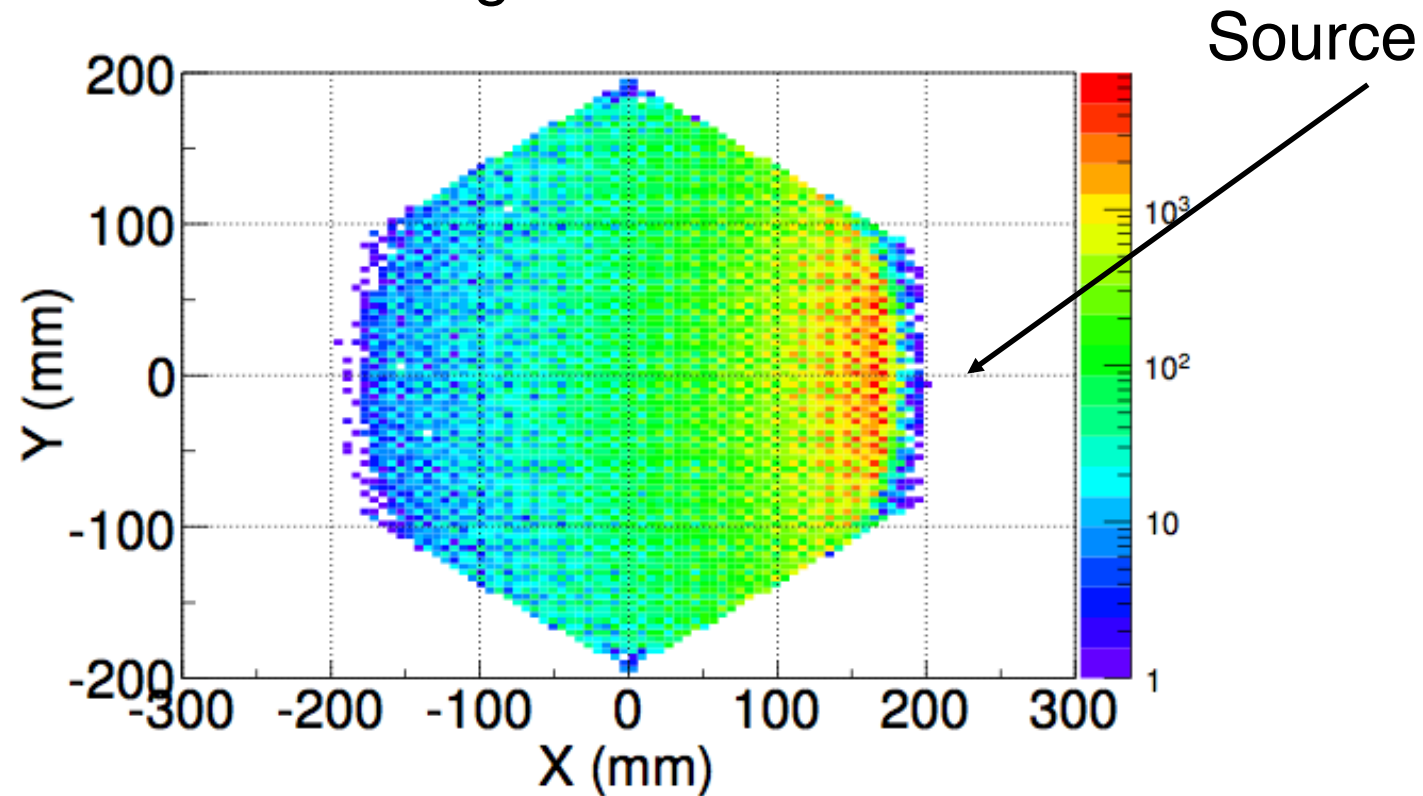
How the detector works



Preliminary design of the nEXO detector in SNOLab's cryopit

Position/multiplicity reconstruction

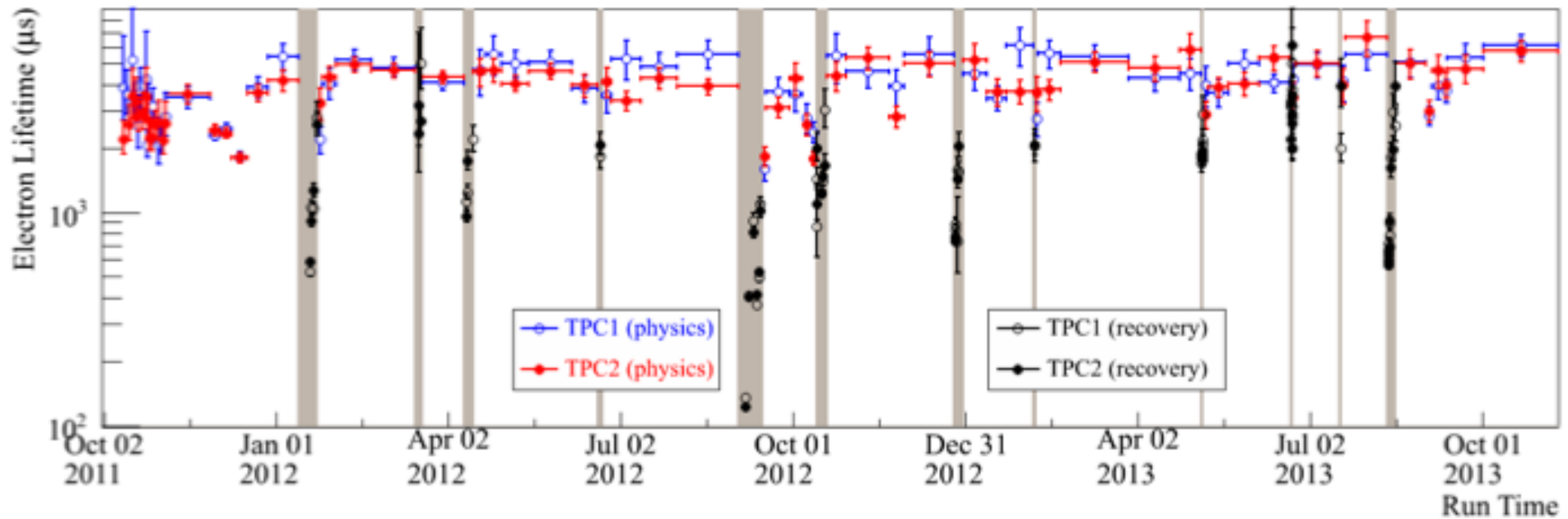
Combine signals into “clusters”



Uncertainty, 2.4 (1.2) mm U (V) + 1.5 mm shift (taken as systematic error), Z (0.5 mm), measured using internal decays on the cathode

Total error in fiducial volume due to position reconstruction: **1.73%**

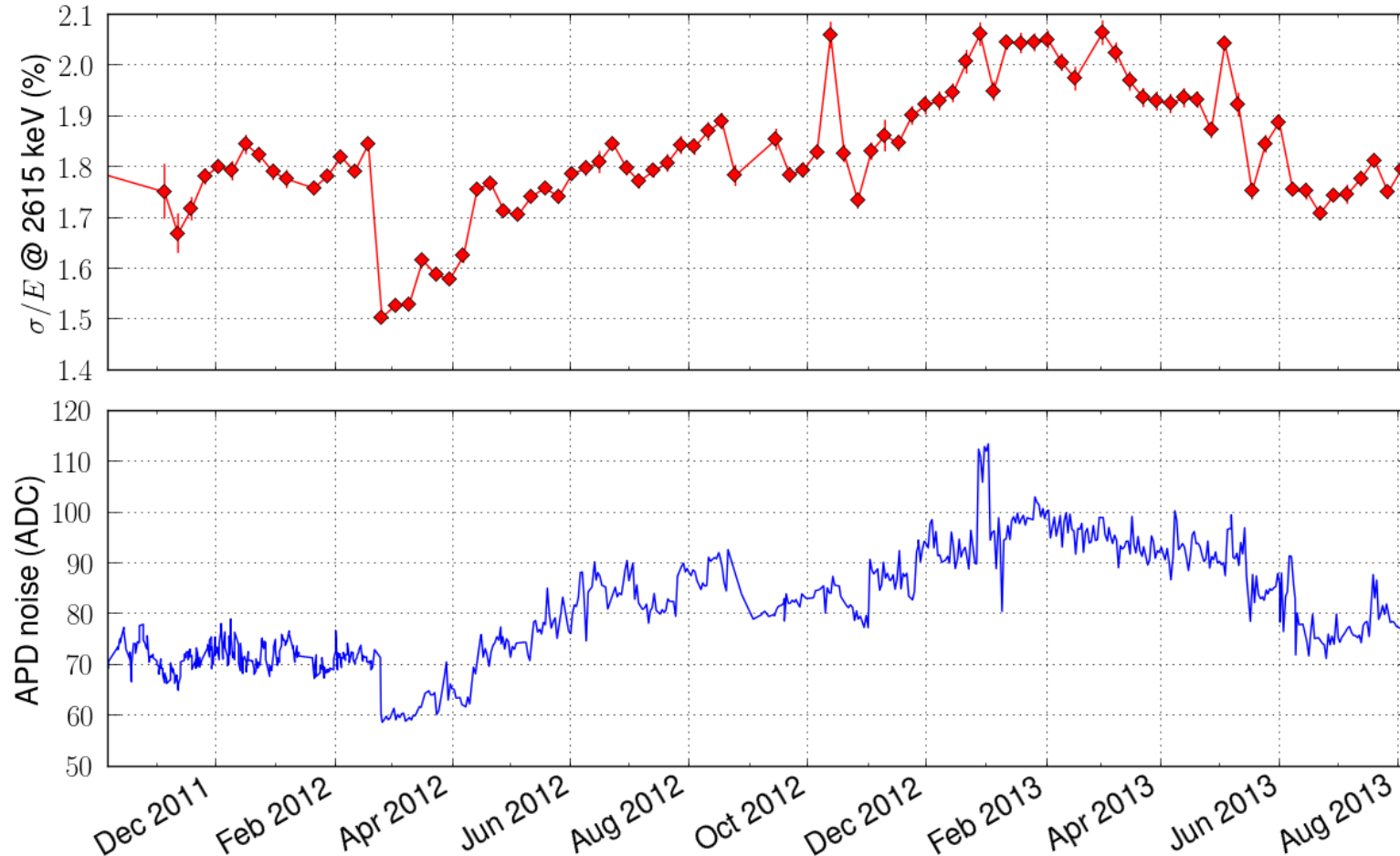
Xe Purity over Run 2



- Estimation based upon data from ^{228}Th source runs
- Purity strongly correlated with circulation pump speed
- At $\tau_e = 3 \text{ ms}$: drift time $< 110 \mu\text{s}$, loss of charge: 3.6% at full drift length

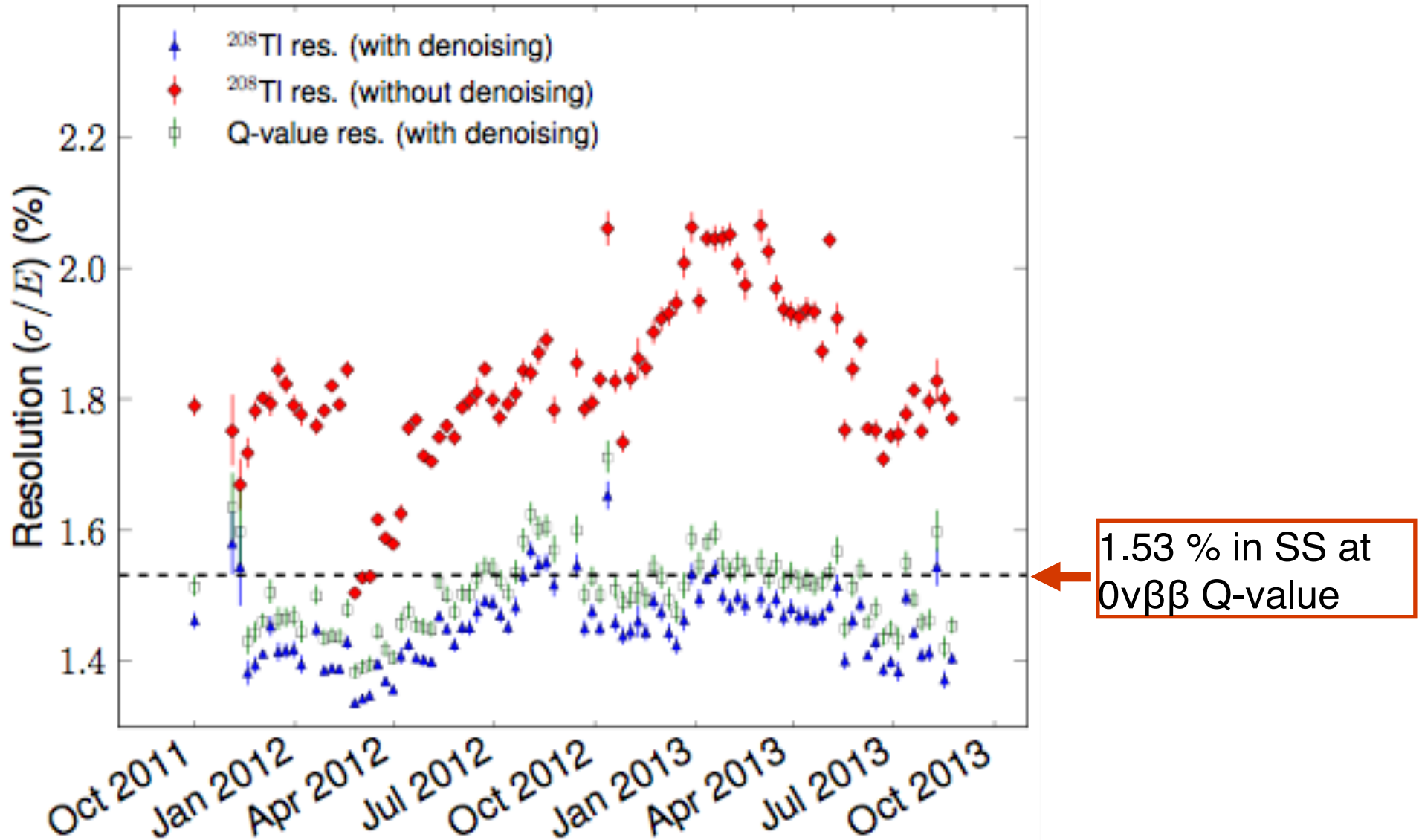
APD Denoising

Problem: Noise and resolution is dependent on the varying (correlated) noise of the APDs



(Current) solution: Find the optimum combination of APD signals *per event*, given position and noise

APD Denoising



Systematic errors

- $0\nu\beta\beta$ detection efficiency:

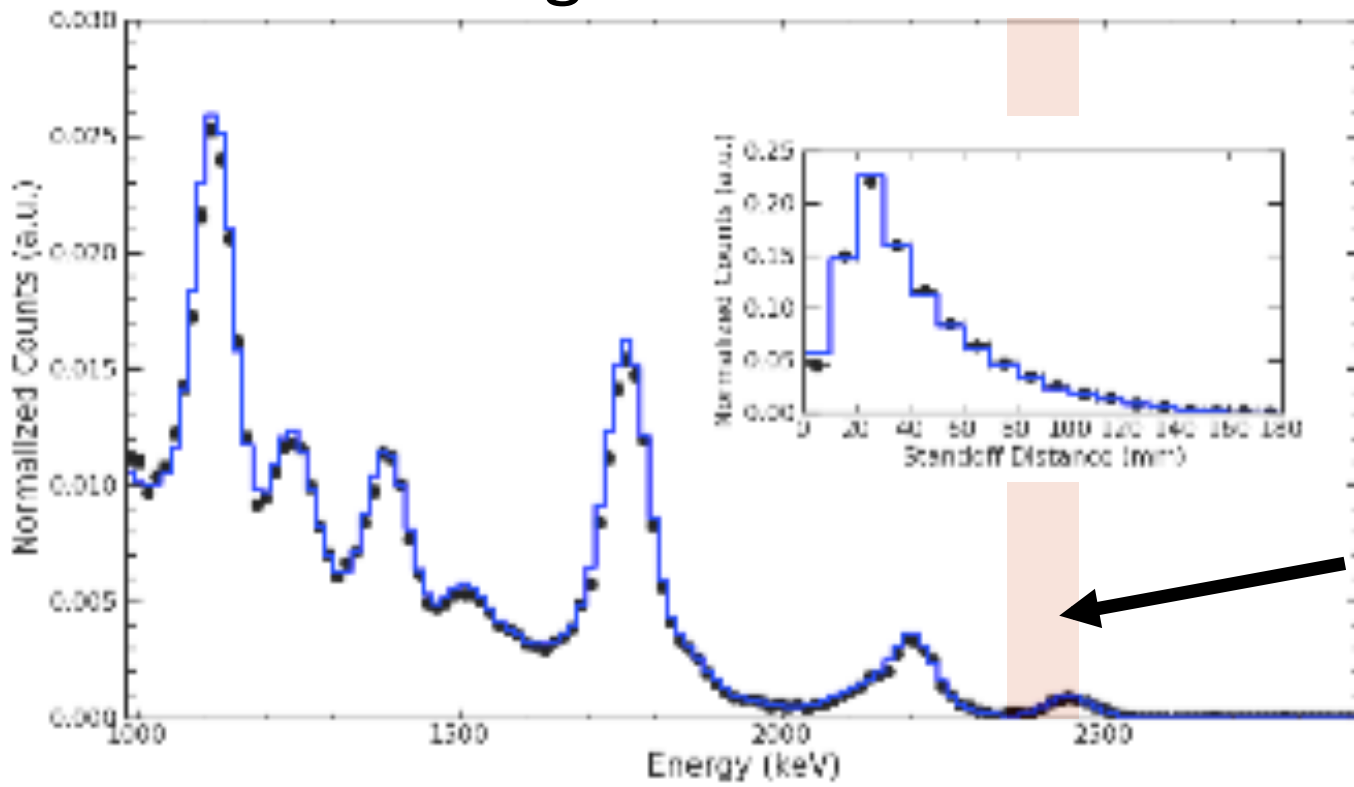
Source:	Signal efficiency [%]:	Relative error [%]:
Summary from PRC 89 , 015502 (2014)	93.1	0.9
Partial reconstruction	90.9	7.8
Fiducial volume/rate agreement		3.4
Total:	84.6	8.6

- Region-of-interest (ROI) backgrounds:

Source:	Relative error [%]:
Background shape distortion	9.2
Choice of background model components	5.7
Variation of energy resolution over time	1.5
Total:	10.9

- Location of $0\nu\beta\beta$ ROI: “ β -scale” allowed to float in fit
 - Deviations between β and γ energy scale: $E_\beta = B \cdot E_\gamma \Rightarrow B = 0.999 \pm 0.002$
- Single-site fraction error: **9.6%** SS/MS fraction allowed to vary within this error in fit

Systematic errors agreement with simulation

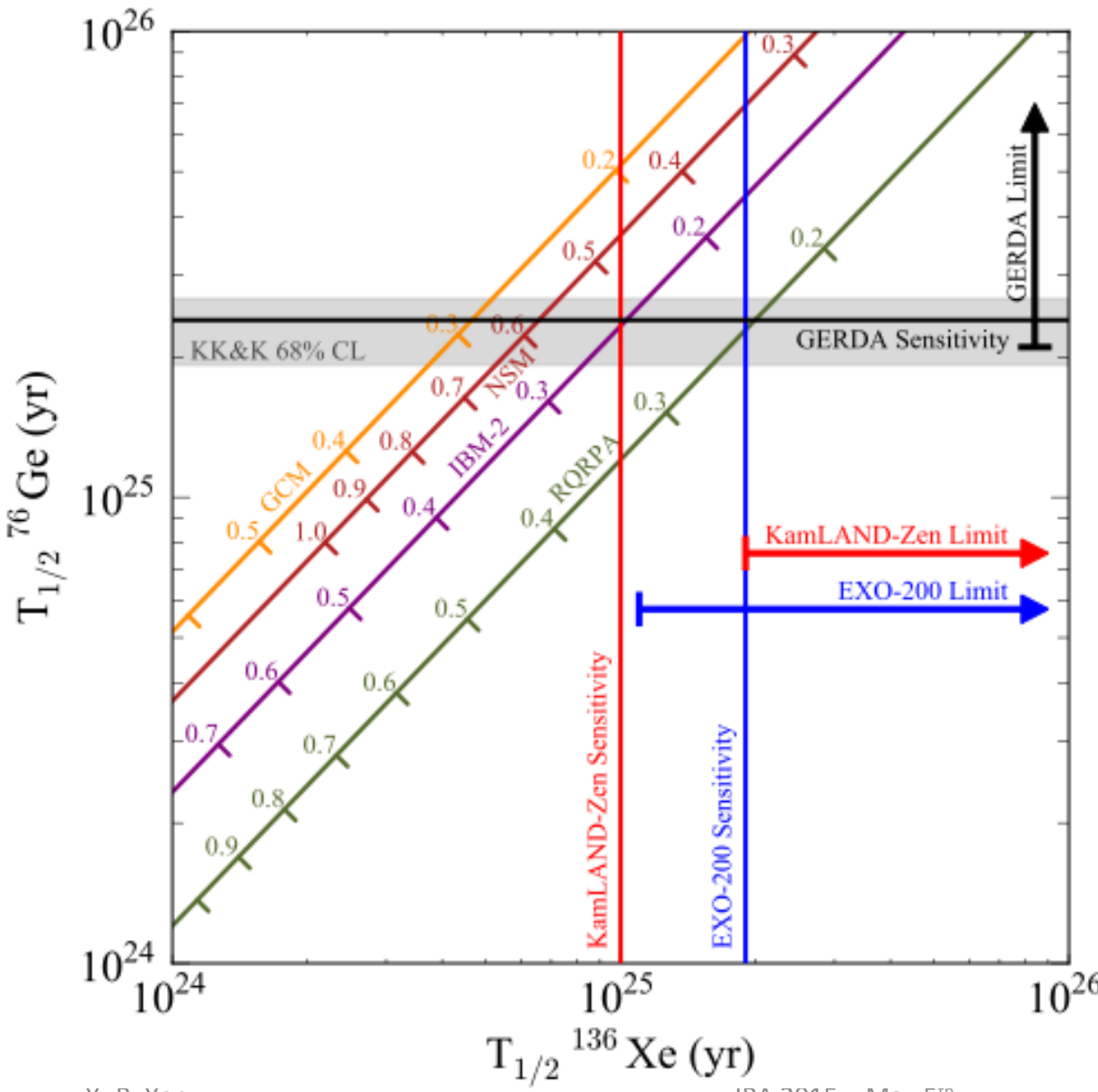


Determine how systematics issues affect background estimates in the ROI.

Allowed background in ROI (red region) to float within this error with respect to the rest of the energy spectrum.

^{226}Ra source data, single-site: example distribution comparison used to estimate systematics (also used ^{228}Th , ^{60}Co , ^{137}Cs sources)

$0\nu\beta\beta$ status comparison



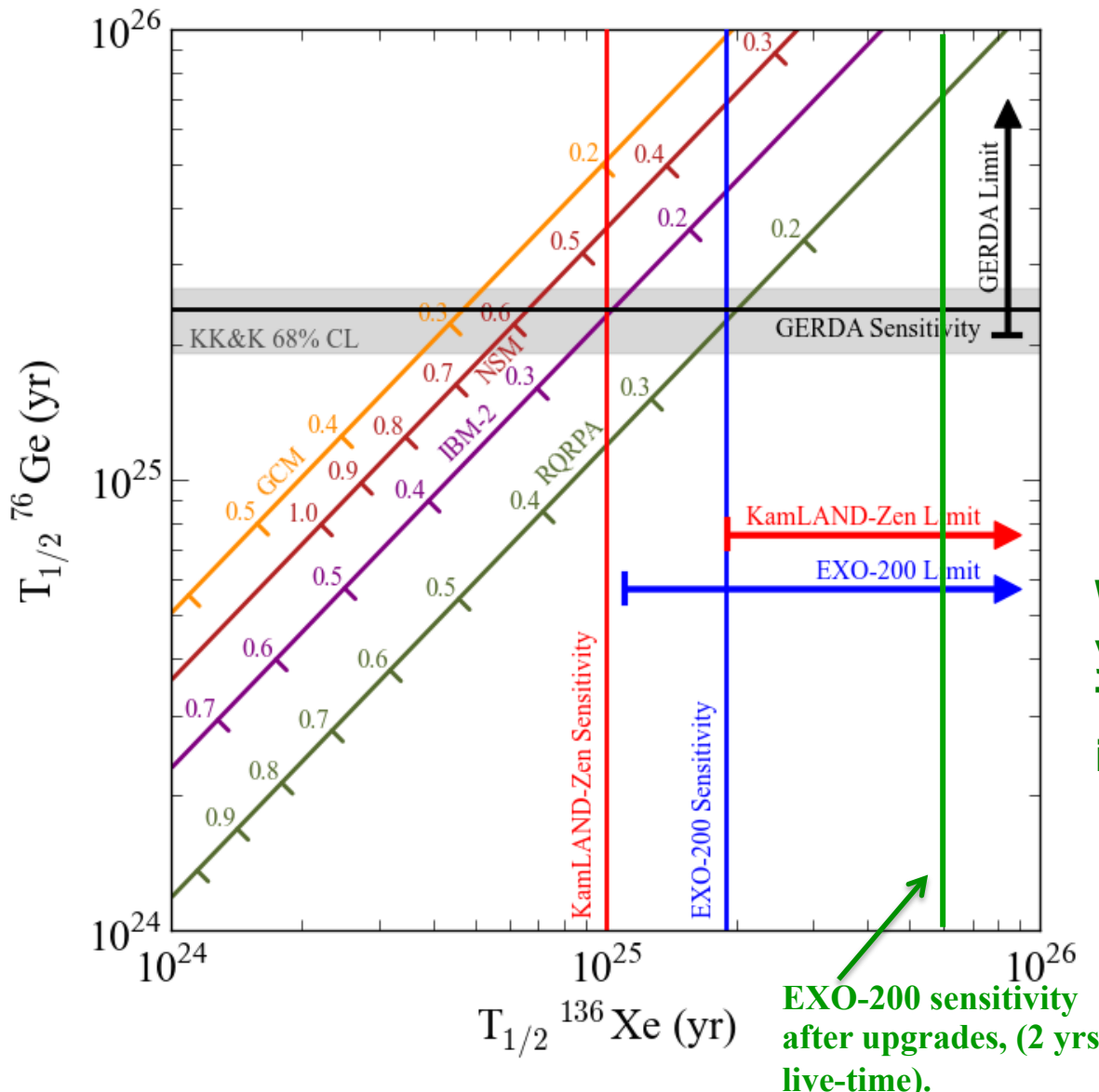
EXO-200:
Nature (2014),
doi:10.1038/nature13432

GERDA Phase 1:
PRL 111 (2013) 122503

KamLAND-Zen:
PRL 110 (2013) 062502

KK&K Claim:
Mod. Phys. Lett., A21
(2006) 1547

EXO-200 $0\nu\beta\beta$ Half-life Sensitivity



$T_{1/2}^{0\nu\beta\beta} > 1.1 \cdot 10^{25} \text{ yr (90\%CL)}$

$\langle m_\nu \rangle < 190 - 450 \text{ meV}$

Median $T_{1/2}^{0\nu\beta\beta}$ sensitivity:
 $1.9 \cdot 10^{25} \text{ yr}$

J.B.Albert et al. (EXO-200), Nature (6 June, 2014)

A. Gando et al. (KamLAND-ZEN), PRL 110 (2013) 062502

M. Agostini et al. (GERDA), PRL 111 (2013) 122503

With upgraded detector and 2 yrs of live-time, EXO-200 $T_{1/2}^{0\nu\beta\beta}$ median sensitivity will increase by a factor of 3.

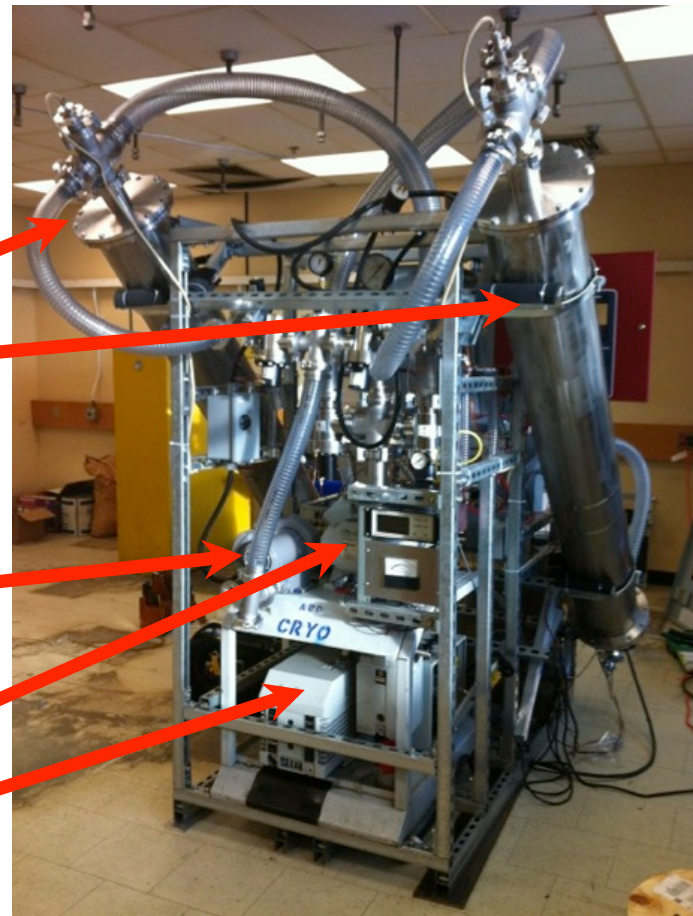
One of the most sensitive $0\nu\beta\beta$ experiments in the next 3 - 5 years.

Radon Background and Deradonator

Analysis indicates that up to 50% of background can be due to Rn in the airgap between the cryostat and the lead shielding. This background can be eliminated by flushing the space with Rn free air.



charcoal-filled columns
(~30 kg each)

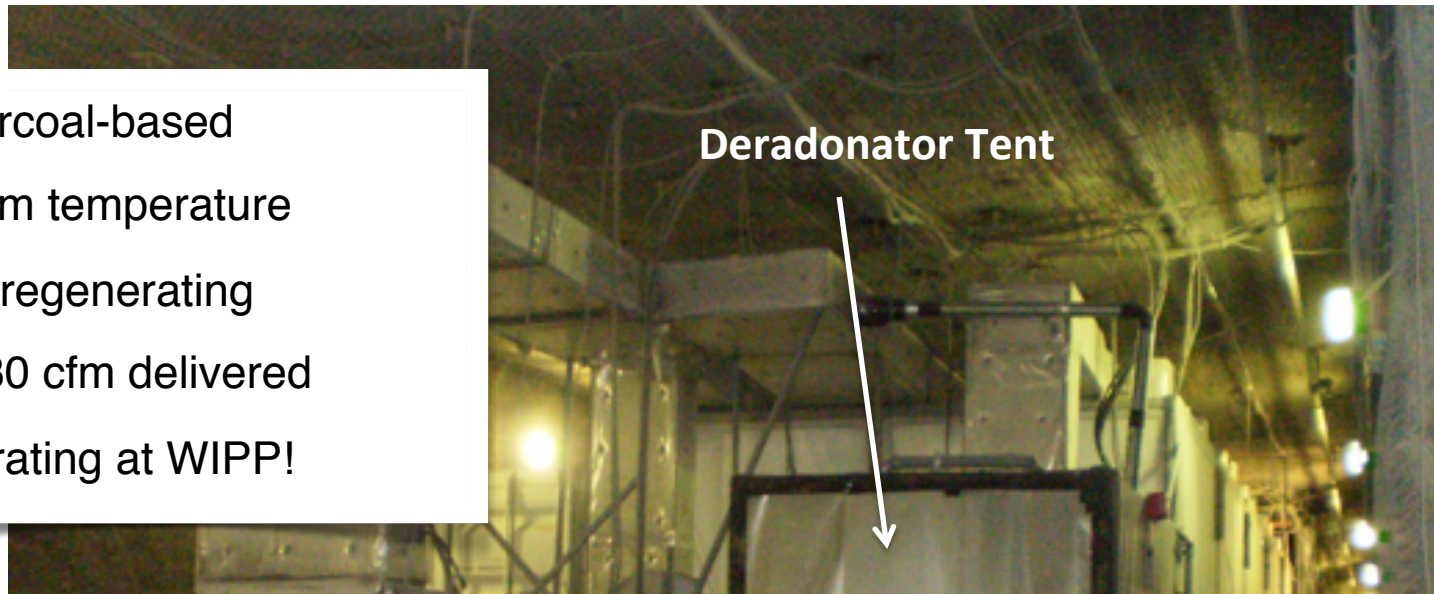


pressure air
blower
(~30 in H₂O)

vacuum pumps:
roots blower
rotary vane

The EXO-200 Deradonator in the Mine

- Charcoal-based
- Room temperature
- self-regenerating
- 10-30 cfm delivered
- operating at WIPP!



Average yearly radon concentration
in the EXO-200 clean room:

~ 6 Bq/m³

Radon in air delivered by the filter:

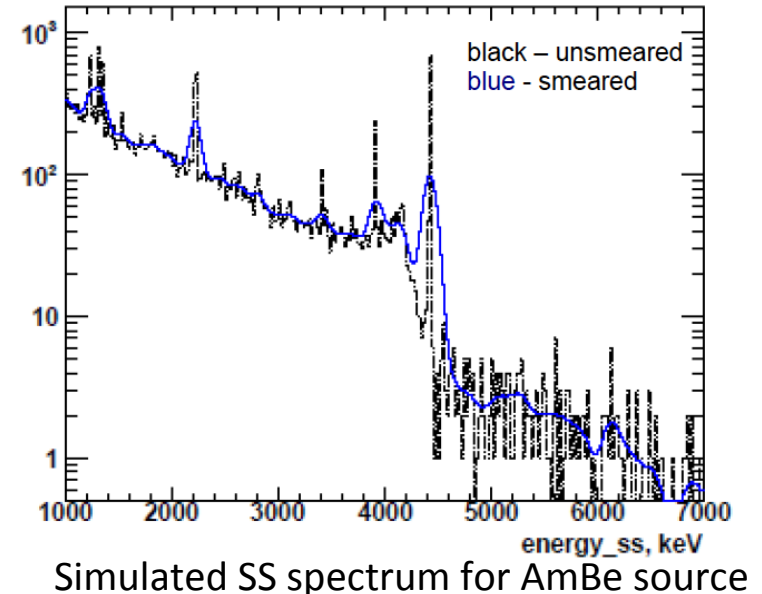
~0.2 Bq/m³

Restart and Re-Commissioning

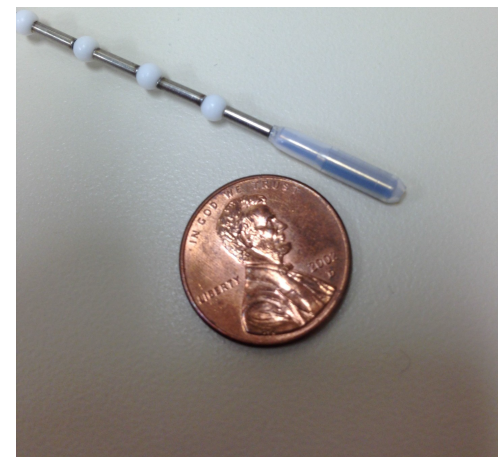
New Calibration Sources

- New AmBe source can provide n-capture gamma calibration at 4.4 MeV.
- Double escape peak can provide a second point for beta line calibration at 3.3 MeV.
- Can produce a controlled sample of ^{137}Xe for beta scale calibration.
- Strong U and Th sources for external background studies.

Improvements to both existing and new data



Simulated SS spectrum for AmBe source



Source capsule passed mechanical tests
43